UC San Diego

UC San Diego Previously Published Works

Title

Multiple Glycosaminoglycan-binding Epitopes of Monocyte Chemoattractant Protein-3/CCL7 Enable It to Function as a Non-oligomerizing Chemokine*

Permalink

https://escholarship.org/uc/item/1vx347r1

Journal

Journal of Biological Chemistry, 289(21)

ISSN

0021-9258

Authors

Salanga, Catherina L
Dyer, Douglas P
Kiselar, Janna G
et al.

Publication Date

2014-05-01

DOI

10.1074/jbc.m114.547737

Peer reviewed

eScholarship.org Powered by the California Digital Library
University of California

THE JOURNAL OF BIOLOGICAL CHEMISTRY VOL. 289, NO. 21, pp. 14896–14912, May 23, 2014
© 2014 by The American Society for Biochemistry and Molecular Biology, Inc. Published in the U.S.A.

Multiple Glycosaminoglycan-binding Epitopes of Monocyte Chemoattractant Protein-3/CCL7 Enable It to Function as a Non-oligomerizing Chemokine*

Received for publication, January 4, 2014, and in revised form, April 2, 2014 Published, JBC Papers in Press, April 11, 2014, DOI 10.1074/jbc.M114.547737

Catherina L. Salanga[‡], Douglas P. Dyer[‡], Janna G. Kiselar[§], Sayan Gupta[§¶], Mark R. Chance[§¶], and Tracy M. Handel[‡1]

From the [‡]Skaggs School of Pharmacy and Pharmaceutical Science, University of California, San Diego, La Jolla, California 92093-0684 and the [§]Center for Proteomics and Bioinformatics and [¶]Center for Synchrotron Biosciences, Case Western Reserve University, Cleveland, Ohio 44106

Background: Chemokines oligomerize upon glycosaminoglycans to establish chemokine gradients.
Results: Monomeric monocyte chemoattractant protein (MCP)-3/CCL7 has a dense network of glycosaminoglycan-binding epitopes that provide sufficient affinity for glycosaminoglycans, but the inability to oligomerize renders it sensitive to glycosaminoglycan density unlike the oligomerizing homolog, MCP-1/CCL2.
Conclusion: Different glycosaminoglycan-binding properties of CCL7 and CCL2 suggest non-redundant functions and regulation.
Significance: Glycosaminoglycan density may regulate the cell surface accumulation of chemokines.

The interaction of chemokines with glycosaminoglycans (GAGs) facilitates the formation of localized chemokine gradients that provide directional signals for migrating cells. In this study, we set out to understand the structural basis and impact of the differing oligomerization propensities of the chemokines monocyte chemoattractant protein (MCP)-1/CCL2 and MCP-3/CCL7 on their ability to bind GAGs. These chemokines provide a unique comparison set because CCL2 oligomerizes and oligomerization is required for its full *in vivo* activity, whereas CCL7 functions as a monomer. To identify the GAG-binding determinants of CCL7, an unbiased hydroxyl radical footprinting approach was employed, followed by a focused mutagenesis study. Compared with the size of the previously defined GAG-binding epitope of CCL2, CCL7 has a larger binding site, consisting of multiple epitopes distributed along its surface. Furthermore, surface plasmon resonance (SPR) studies indicate that CCL7 is able to bind GAGs with an affinity similar to CCL2 but higher than the non-oligomerizing variant, CCL2(P8A), suggesting that, in contrast to CCL2, the large cluster of GAG-binding residues in CCL7 renders oligomerization unnecessary for high affinity binding. However, the affinity of CCL7 is more sensitive than CCL2 to the density of heparan sulfate on the SPR surfaces; this is likely due to the inability of CCL7 to oligomerize because CCL2(P8A) also binds significantly less tightly to low than high density heparan sulfate surfaces compared with CCL2. Together, the data suggest that CCL7 and CCL2 are non-redundant chemokines and that GAG chain density may provide a mechanism for regulating the accumulation of chemokines on cell surfaces.

In addition to chemokine activation of chemokine receptors, interactions of chemokines with glycosaminoglycans (GAGs)[2] have been increasingly recognized as an important functional component of their activity. The interaction of chemokines with GAGs provides a mechanism for localizing and concentrating them at specific anatomical sites, and possibly for presenting the ligands to their chemokine receptors. Additionally, GAG interactions have been reported to be involved in secretion of chemokines from cells (1) and transcytosis of chemokines produced in one compartment such as the extravascular space, across cells where they encounter receptor-bearing leukocytes in another compartment such as the bloodstream (2, 3). Chemokine-GAG interactions may even promote intracellular signaling, independent of chemokine receptors, as demonstrated for RANTES/CCL5 binding to the GAG chains of CD44 (4). Proudfoot and colleagues (5) first demonstrated the requirement of GAG binding for chemokine-induced cell migration *in vivo*, and these findings have been further supported with similar studies of other chemokines in recent years (6–8). In these initial studies, GAG binding-deficient variants of several chemokines (MCP-1/CCL2, MIP-1β/CCL4 and CCL5) were found to promote chemokine-induced migration *in vitro*, but exhibited a dramatic reduction in their ability to recruit cells *in vivo*, compared with the wild-type (WT) counterparts (5). Although chemokine monomers are known to activate receptors (9, 10), in previous studies (5, 11), oligomerization was also shown to be required for *in vivo* function of the same chemokines and hypothesized to be relevant to their interactions with GAGs in some *in vivo* models of cell migration.

Given the established importance of chemokine interactions with GAGs, there has been a growing interest in defining their GAG-binding epitopes. This information has been used to gen-

* This work was supported, in whole or in part, by National Institutes of Health Grants R01 AI37113 (to T. M. H.), R01 EB09998 and P30 EB09688 (to M. R. C.), a Ruth L. Kirschstein NIGMS MARC Predoctoral Fellowship (F31) (to C. L. S.), and National Institute for Biomedical Imaging and Bioengineering Grants P30-EB-09998 and R01-EB-09688 (to S. G.).
[1] To whom correspondence should be addressed: 9500 Gilman Dr., MC0684, La Jolla, CA 92093. Tel.: 858-822-6656; Fax: 858-822-6655; E-mail: thandel@ucsd.edu.

[2] The abbreviations used are: GAG, glycosaminoglycan; CCR, CC-type chemokine receptor; CCL, CC-type chemokine ligand; CXCL, CXC-type chemokine ligand; HS, heparan sulfate; SPR, surface plasmon resonance; MCP, monocyte chemoattractant protein.

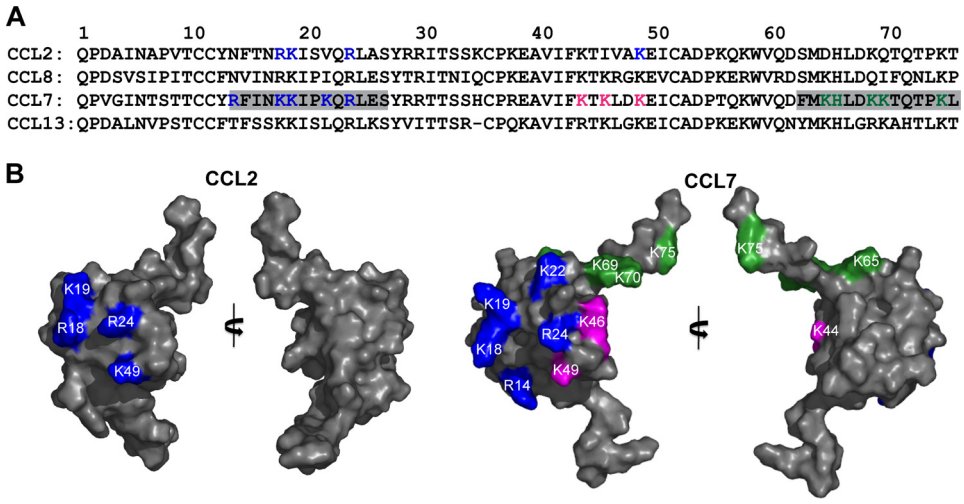

FIGURE 1. **Sequence alignment of the MCP family of chemokines and GAG-binding epitopes of MCP-1/CCL2 and MCP-3/CCL7.** *A*, sequence alignment of MCP-1/CCL2, MCP-2/CCL8, MCP-3/CCL7, and MCP-4/CCL13. Basic residues involved in GAG binding are highlighted in *blue* in the CCL2 sequence. Peptides-(13–27) and -(63–76), which exhibited a decrease in oxidation rate when GAG was present, are shaded *gray* in the CCL7 sequence. CCL7 GAG recognition sites are highlighted by region: *blue* (N-loop), *magenta* (40s loop), and *green* (C-terminal tail) on CCL7. *B*, GAG-binding epitopes mapped onto the monomer structure of CCL2 (*left*) and CCL7 (*right*) in two different views.

erate GAG binding-deficient chemokines, which in turn allows study of the functional role of GAG interactions in a chemokine-specific manner. Furthermore, identification of the common as well as unique features of the GAG-binding epitopes and how they present on chemokine surfaces in the context of monomeric and oligomeric structures is gradually providing insight into general mechanisms of chemokine-GAG recognition as well as the potential for specificity in the interactions (12, 13). For example, MIP-1α/CCL3, CCL4, and CCL5 all contain a GAG-binding motif predominantly in the 40s loop region (14–16). By contrast, IL-8/CXCL8 has been shown to bind GAGs mainly through its C-terminal α-helix (17) and ITAC/CXCL11 through a diffuse epitope involving the 50s loop and Lys-17 (18). However, even when similar epitopes are identified, there can be significant differences in the overall GAG-binding site in the context of oligomeric species, which are often induced upon GAG binding (19). For example, CCL3 and CCL4, which have an overall acidic isoelectric point, form double-helical polymers (20), whereas CCL5, which has a basic isoelectric point, forms a more linear polymer (21) such that the 40s loop GAG-binding epitopes have different spatial distributions on the surface of the two polymer types. Overall, these structural differences suggest the potential for specificity in chemokine-GAG interactions. Although such specificity remains an open question, if significant, it could provide a powerful mechanism for precise control of chemokine localization and accumulation, and in turn cell migration and other chemokine-relevant functions.

MCP-3/CCL7 belongs to the monocyte chemoattractant protein (MCP) subfamily of chemokines, which include MCP-1/CCL2, MCP-2/CCL8, MCP-3/CCL7, and MCP-4/CCL13 in humans. All have a high level of sequence identity ranging from ~56 to 71% (Fig. 1*A*) and all bind to the chemokine receptor CCR2. However, CCL7, CCL8, and CCL13 are also ligands of CCR1, CCR3, and CCR5 (22–24). Because of its broad recognition of receptors, CCL7 can activate many different cell types such as monocytes, eosinophils, basophils, and T cells (25). Furthermore, unlike CCL2 and CCL8, which oligomerize in solution and more avidly in the presence of GAGs (11, 26), NMR studies indicate that CCL7 is monomeric even at a concentration of ~2 mM (27), and mass spectrometry data suggest that it also does not oligomerize in the presence of heparin (26). Nevertheless, whereas non-oligomerizing variants of CCL2, CCL4, and CCL5 are impaired in their ability to recruit cells *in vivo*, at least in part because of impaired interactions with GAGs, CCL7 is functional as a monomer (5, 7). However, like these other chemokines, it requires interactions with GAGs to promote cell migration *in vivo* (7).

Given their high sequence homology (71% identity, 76% similarity, Fig. 1*A*) but distinct oligomerization propensities, we became interested in the mechanisms by which CCL7 and CCL2 interact with GAGs, to understand why CCL2 requires oligomerization, why CCL7 does not, and the impact of these differences on their affinity and specificity for GAGs. In this study, we show that CCL7 has a larger network of GAG-binding residues than CCL2, likely explaining its ability to function as a monomeric chemokine. As a consequence, the binding affinity of CCL7 and CCL2 is similar for heparin and heparan sulfate (HS), whereas a non-oligomerizing variant of CCL2, CCL2(P8A), has a lower affinity for both GAGs. However, SPR data show that the affinity of monomeric CCL7 is more sensitive than CCL2 to the density of HS GAG chains, strongly suggesting the necessity of CCL2 oligomerization for high affinity interaction with GAGs. Interestingly, we also show that heparin and HS favor different oligomeric species for CCL2. Taken together, these findings reveal distinct mechanisms in which these two chemokines recognize GAGs, based on their inherent differences in oligomerization and pattern of GAG-binding residues.

EXPERIMENTAL PROCEDURES

Chemokine Expression and Purification

CCL2 and CCL7 were subcloned into the pHUE construct (kindly provided by Rohan T. Baker) and expressed as a His-

ubiquitin fusion protein as described previously (28). Briefly, CCL7 was solubly expressed in BL21(DE3)pLysS *Escherichia coli* cells grown at 30 °C. Cells were induced with isopropyl-β-D-thiogalactopyranoside at an optical density ~0.4 and harvested after 3 h. Protein was purified with nickel-Sepharose affinity chromatography using an ÄKTA FPLC (GE Healthcare), and then passed over a reversed-phase high-pressure liquid chromatography (HPLC) C18 semi-prep column. To obtain CCL7, the fusion protein was cleaved with 1:100 (chemokine: ubiquitinase, molar ratio) ubiquitinase for 3 h at room temperature, passed over nickel-nitrilotriacetic acid affinity chromatography to remove unwanted cleavage products followed by a final HPLC purification step. Protein identity and purity was confirmed by electrospray ionization mass spectrometry. CCL2 was insolubly expressed as inclusion bodies in BL21(DE3)pLysS *E. coli* cells grown at 37 °C, induced with isopropyl-β-D-thiogalactopyranoside at an optical density ~0.6–0.8 and grown for 3 h before being harvested. Inclusion body pellets were purified by nickel-nitrilotriacetic acid chromatography, refolded with Hampton Fold-it Buffer number 11 (FoldIt Screen, Hampton Research), concentrated with a 10-kDa MWCO filter followed by dialysis into ubiquitinase cleavage buffer (20 mM Tris, pH 8, 200 mM NaCl). The CCL2 fusion was then cleaved with ubiquitinase and purified in the same manner as CCL7. Alanine mutants were generated by QuikChange site-directed mutagenesis (Stratagene) and mutants were purified in the same manner as the WT protein.

Hydroxyl Radical Footprinting Analysis by Mass Spectrometry of MCP-3/CCL7 in Complex with Heparin

In overview, CCL7, alone or in complex with heparin octasaccharide (dp8, Neoparin), was exposed to x-rays for various time points ranging from 0 to 10 ms. High flux x-ray exposure of protein for millisecond time points results in modest amounts of oxidative modification of solvent-accessible side chains and limits secondary modifications such as backbone cleavage and unfolding (29). Irradiated samples were pepsin digested and the peptides were detected by reversed-phase liquid chromatography coupled with tandem mass spectrometry (LC-MS/MS). Oxidatively modified peptides were detected using the ProtMapMS software package, manually validated, and the rates of oxidation of peptides over time were compared between CCL7 in complex or alone as has been described previously (30). Details are provided below.

Radiolysis—CCL7 was prepared with 10 mM sodium cacodylate buffer (pH 7.2) to a final concentration of 10 μM. Using a flow setup, samples were exposed to the X-28C beamline of the National Synchrotron Light Source (Brookhaven National Laboratory) for 0, 2.5, 5, and 10 ms in the presence or absence of heparin octasaccharide at a 1:2 molar ratio (chemokine:heparin) with beam currents ranging from 210 to 253 mA. All experiments were carried out at ambient temperature. Following exposure, free hydroxyl radicals were quenched with 10 mM methionine-NH_2 and the samples were stored at −80 °C.

Proteolysis—Irradiated samples were diluted 5-fold in 25 mM ammonium bicarbonate buffer (pH 8.2) reduced with DTT to a final concentration of 10.5 mM for 20 min at 60 °C and alkylated with iodoacetamide to a final concentration of 100 mM for 30 min at room temperature in the dark. Samples were then acidified with 1 M HCl to pH ~ 2 and digested with freshly prepared porcine pepsin (Worthington) in 0.1% trifluoroacetic acid to a 1:5 ratio (w/w) of pepsin:chemokine for 24 h at room temperature and then frozen at −20 °C to terminate the pepsin reaction. To remove excess salts, digested samples were passed over 50-mg Sep-Pak C18 cartridges (Waters Corp.), washed with 1% acetic acid, eluted with 80% acetonitrile (ACN), 0.1% acetic acid and lyophilized. Pepsin digestion of CCL7 resulted in greater than 72% sequence coverage from replicate experiments.

LC-MS/MS—For mass spectrometric analysis, ~1 pmol of digest was loaded onto a Dionex reversed-phase HPLC system. Peptides were separated with a 15 cm × 75 μm (3 μm, 100 Å) Acclaim PepMap100 C18 column (Dionex) using a linear gradient of 5–50% B over 60 min (Buffer A: 20% ACN, 0.1% formic acid; Buffer B: 80% ACN, 0.1% formic acid). Mass spectrometry data were acquired in positive mode on a LTQ-FT mass spectrometer (Thermo Fisher Scientific) equipped with a nanospray ion source using a spray voltage of 2 kV. Mass spectra were collected in a data-dependent manner where the eight most abundant peptide ions were selected and subsequently fragmented by collision-induced dissociation to produce MS/MS ion fragmentation (31).

Data Processing and Analysis—Data were processed using the ProtMapMS software package (30), and manually validated using Xcalibur (Thermo Scientific). Proteolytic fragments (modified and unmodified) were separated by LC-MS/MS and the extent of modification for select peptides was calculated by integration of peak area, extracted from the total ion current chromatograms, and compared across various exposure times. The fraction of unmodified peptide was quantified as the fraction of unmodified peptide to the total amount of peptide (modified and unmodified). The fraction of unmodified peptide was then plotted as a function of time (ms) in a pseudo-first order rate reaction to determine the rate of oxidation using the equation, $y = e^{-kt}$ (where k = rate constant, t = exposure time). Interpretation of the changes in oxidation rates for peptides generated from protein in complex generally correlate with changes in solvent accessibility and protection from modification as a result of binding events or conformational changes. The specific sites of modification for each peptide were manually assigned using tandem MS spectra. Solvent accessibilities of candidate GAG-binding residues in protected peptides identified by the radiolytic footprinting method were calculated using the VADAR program (PENCE, University of Alberta) using the CCL7 structure (PDB ID 1BO0).

Validation of Mutants with Heparin-Sepharose Binding Assays

Fifty micrograms of WT or mutant protein was loaded onto either a 1-ml HiTrap Heparin HP column (GE Healthcare) or a 1-ml HiTrap SP HP column (GE Healthcare) connected to an ÄKTA FPLC system (GE Healthcare). Samples were eluted over a linear gradient of 0–2 M NaCl in 10 mM sodium phosphate (pH 7.2) at a flow rate of 0.5 ml/min. The amount of NaCl required to elute protein was determined by the %B required to elute each sample; protein elution was monitored by absorbance at 280 nm. The assay was run in triplicate for each protein. To determine the effects of alanine mutations on heparin bind-

ing, the difference in the concentration of NaCl required to elute WT *versus* mutant protein was calculated according to Equation 1.

$$\Delta[\mathrm{NaCl}]_H = [\mathrm{NaCl}]_{H,WT} - [\mathrm{NaCl}]_{H,mutant} \quad \text{(Eq. 1)}$$

The difference in the concentration of NaCl required to elute WT *versus* mutant protein from SP-Sepharose resin was also calculated (Equation 2).

$$\Delta[\mathrm{NaCl}]_S = [\mathrm{NaCl}]_{S,WT} - [\mathrm{NaCl}]_{S,mutant} \quad \text{(Eq. 2)}$$

The specificity index was then calculated by Equation 3.

$$\Delta\Delta[\mathrm{NaCl}] = \Delta[\mathrm{NaCl}]_H - \Delta[\mathrm{NaCl}]_S \quad \text{(Eq. 3)}$$

Surface Plasmon Resonance

Biotinylation of GAGs—HS from bovine kidney (Sigma) was resuspended at 5 mg/ml in 100 mM MES (pH 5.0) before addition of 6.5 mM EDC (GE Healthcare) and 1.25 mM EZ-Link Hydrazide-LC-Biotin (Pierce); the solution was then incubated overnight at room temperature with rotation. Excess biotin was removed by extensive dialysis into water using a 0.5–1-kDa cut-off float-a-lyzer (Spectrum Labs) and then stored at 4 °C. Biotinylated porcine intestinal heparin (average molecular mass = 15 kDa) was purchased from Calbiochem.

Surface Plasmon Resonance Analysis—Kinetic analysis of chemokine-GAG interactions was done by SPR using a BIAcore 3000 instrument (BIAcore) with a C1 sensor chip. The C1 sensor chip was prepared by activation with a 1:1 mixture of NHS and EDC (300 μl at 20 μl/min), immobilization of Neutravidin (Invitrogen) at 20 μl/min in 10 mM NaOAc (pH 6), deactivation of excess groups with ethanolamine, and then washing the surface with 10 mM NaOAc (pH 5.5) buffer prior to GAG addition. To address the effects of GAG density on chemokine-GAG binding affinities, 0.2 mg/ml of GAG was added at various levels of saturation based on response units. Signals were 47, 250, 140, and 106 response units for heparin and high, medium, and low HS density surfaces, respectively; these numbers represent the actual response units with the exception of 140, which was estimated due to baseline drift. For kinetic analysis, varying concentrations of chemokine (typically 25–1000 nM, unless otherwise stated) were applied to the chip for 5 min at 40 μl/min in SPR running buffer (10 mM HEPES, 150 mM NaCl, 3 mM EDTA, 0.05% Tween 20, pH 7.4), followed by 5 min of dissociation. Surfaces were regenerated after each injection using 0.1 M glycine, 1 M NaCl, and 0.1% Tween 20 (pH 9.5) (32). All data were analyzed with the BIAevaluation software (BIAcore) using a 1:1 Langmuir association model and steady state analysis (GE Healthcare).

Chemical Cross-linking of Chemokine with GAG

Chemical cross-linking was performed by incubating chemokine with varying concentrations of heparin octasaccharide (Neoparin) or HS from bovine kidney (Sigma) in 50 mM HEPES (pH 7.2) for 30 min at room temperature. Sulfoethyleneglycolbis-(sulfosuccinimidylsuccinate) (Sulfo-EGS, Pierce) was then added to a final concentration of 5 mM, the mixture was allowed to incubate for 30 min and then quenched with 1 M Tris. Samples were resolved on an 18% SDS-PAGE gel. Results shown are representative images of experiments performed in triplicate.

Cell Migration

Migration assays were performed using 24-well transwell plates with 5-μm pore size filter inserts (Corning). Filters were coated with 10 μg/ml of fibronectin (Sigma), seeded with human pulmonary artery endothelial cells (Invitrogen) (100,000 cells per filter), and incubated for 2 days at 37 °C, 5% CO_2. Blood was obtained from the San Diego Blood Bank and peripheral blood mononuclear cells were isolated by Ficoll-Paque density gradient centrifugation. Monocytes were freshly isolated from peripheral blood mononuclear cells by CD14 positive selection using the magnetic assisted cell sorting system (Miltenyi Biotec). WT and mutant protein stocks were diluted into the bottom well at varying concentrations (*e.g.* 0.1–250 nM) using migration buffer (RPMI 1640 + 10% FBS, 10 mM HEPES) in a total volume of 600 μl. Monocytes were resuspended at a concentration of 2.5×10^6 cells/ml in migration buffer and 100 μl of cells were distributed into the upper chamber of each well. Wells with no chemokine were used to account for background migration and wells with cells only (no filter) were used to quantify maximal migration. Cells were allowed to migrate for 2 h at 37 °C in 5% CO_2 after which time cells that migrated to the bottom chamber were counted on a Guava EasyCyte 8HT flow cytometer (EMD Millipore) by counting the number of events in 30 s. Migration was normalized to background migration (no chemokine added) and plotted as the percent of cells migrated to the total number of cells possible (no filter). Data were plotted using GraphPad Prism (GraphPad software) and is shown as the mean ± S.E. from three independent experiments, each performed in at least duplicate.

Detection of Chemokine on Endothelial Cells

EA926 cells (kind gift of the Shyy lab, University of California, San Diego) were resuspended at 0.1×10^6 cells/ml in DMEM + 10% FBS (Invitrogen) and seeded at 20,000 cells/well in a black, clear-bottom 96-well assay plate (Corning) precoated with 0.1 μg/ml of PureCol (Advanced Biomatrix) and allowed to grow overnight at 37 °C in 5% CO_2. Cells were washed twice with PBS + 1 mM $CaCl_2$ + 0.5 mM $MgCl_2$ (cPBS) and then incubated with the indicated concentrations of chemokine in cPBS for 1 h at 37 °C in 5% CO_2. Unbound chemokine was removed by washing with cPBS followed by fixation with 4% paraformaldehyde in PBS (Sigma). For chemokine detection, cells were blocked with Odyssey blocking buffer (LI-COR) for 1 h at room temperature, incubated with 1 μg/ml of anti-CCL2 (R&D) or anti-CCL7 (R&D) for 1 h, washed four times with PBS + 0.05% Tween 20, stained with 1:5000 secondary anti-goat 800CW (LI-COR) in Odyssey blocking buffer, and then signal detected by an Odyssey Infrared Imaging System (LI-COR) (settings: 169 μm resolution, medium quality, 4 mm offset, intensity level 5 for 800 nm detector). Data were plotted using GraphPad Prism (GraphPad software) and shown as the average of three independent experiments (±S.E.) performed in at least duplicates. Statistical significance was performed using a one-way analysis

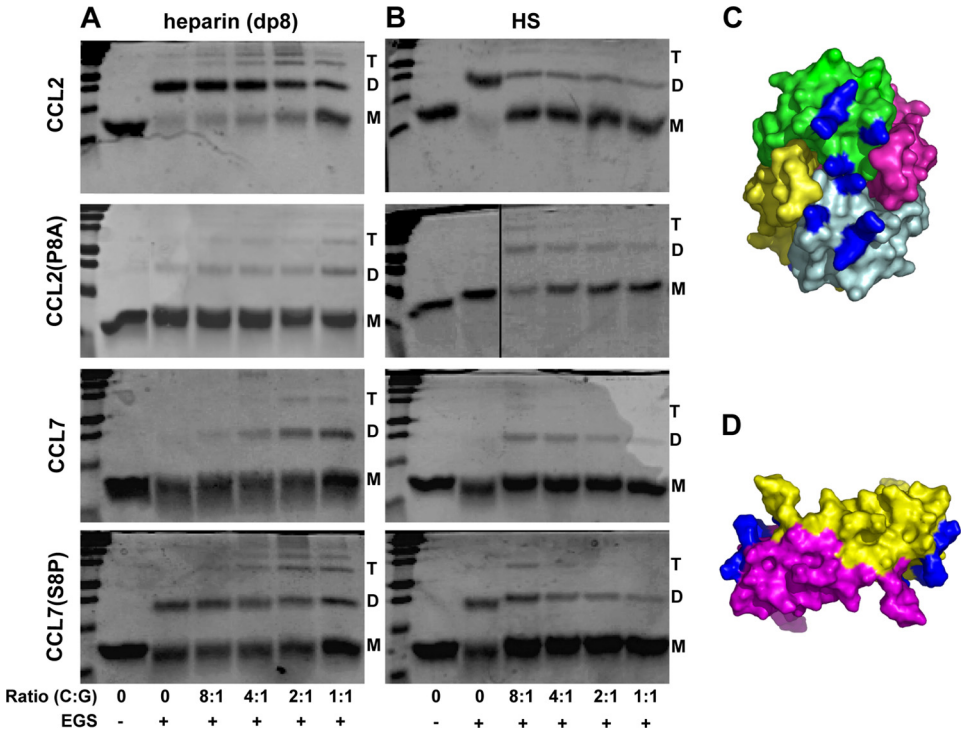

FIGURE 2. **Chemical cross-linking of CCL2, CCL2(P8A), CCL7, and CCL7(S8P) with heparin octasaccharide or HS.** Chemokine (10 μM) was mixed with increasing concentrations of heparin octasaccharide (*A*) or HS (*B*) followed by cross-linking with Sulfo-EGS and formation of oligomeric species was evaluated by SDS-PAGE. Tetramer (*T*), dimer (*D*), and monomer (*M*) species are indicated. *C* and *D*, structures of CCL2 with known GAG-binding epitopes highlighted in *blue* illustrate the potential complementarity between heparin and HS with the different oligomeric structures of CCL2. *C*, the structure of CCL2 shows a continuous linear band of GAG-binding sites (highlighted in *blue*) in the context of the tetramer (PDB code 1DOL), which is stabilized by binding to highly sulfated heparin chains (11). *D*, the dimer structure of CCL2 (PDB code 1DOM) with basic GAG-binding patches (highlighted in *blue*), spatially separated by a relatively charge-neutral area of the dimer structure, is stabilized by HS. HS chains generally consist of unsulfated *N*-acetylated domains flanked by sulfated domains that may complement the dimer structure (55, 57), in contrast to the more uniformly sulfated heparin, which stabilizes the tetramer structure.

of variance (Bonferroni post test) with values indicated as: *, $p < 0.05$; **, $p < 0.01$; ***, $p < 0.001$.

RESULTS

CCL7 Does Not Oligomerize on GAGs, in Contrast to CCL2—Although CCL7 is known to be a monomer in solution (27), it is possible that it can still oligomerize on GAGs, thereby explaining its ability to bind GAGs and function comparably to CCL2 *in vivo*. In previous studies (26, 33) using mass spectrometry, CCL7 was shown to form a 1:1 complex with heparin and HS, whereas CCL2 and CCL8 form dimers in the presence of these GAGs. However, as these data were collected in the gas phase, we sought to evaluate the ability of CCL7 to oligomerize on GAGs in solution.

As previously demonstrated, chemical cross-linking of chemokine in the presence of GAG, whereas not very quantitative, provides a simple method to detect the presence of oligomers (11). In these prior studies, we first showed by analytical centrifugation that in the presence of heparin octasaccharide, CCL2 forms a tetramer (11), likely resembling the tetramer structure observed by crystallography (34), whereas it is a dimer in solution (9, 11) (Fig. 2, *C* and *D*). We then cross-linked CCL2 in the presence of heparin octasaccharide (11), and obtained similar results to those in Fig. 2*A*. The cross-linking revealed the presence of dimers, tetramers, as well as higher order species (presumably dimers of tetramers) reinforcing the analytical centrifugation results. By comparison to the analytical centrifugation data, however, the intensities of the tetramers and higher order oligomer bands significantly underestimate the actual amount of tetramers in the sample due to the reduced probability of having proximal Lys for cross-linking with increasing oligomer size, and because many Lys are protected by their interaction with heparin. Nevertheless, cross-linking serves as a useful method for detecting the propensity of chemokines to oligomerize.

Accordingly, we conducted similar cross-linking experiments with CCL7 in the presence of heparin (Fig. 2*A*). In contrast to CCL2, CCL7 remains largely monomeric. There is slight evidence of some dimer species formed at higher GAG ratios, but this is likely due to two non-oligomerized chemokines in close proximity and cross-linked on the same GAG chain or between chains, similar to that seen with CCL2(P8A) (11) (Fig. 2*A*). Also, given that CCL7 is more enriched with available Lys than CCL2 (Fig. 1), and that these residues are less protected from cross-linking due to a lack of oligomerization in the presence of GAGs, the possibility of these species being nonspecific is more likely. Here the important thing to note is the markedly different behavior of CCL7 compared with CCL2. These conclusions are consistent with the previously reported mass spectrometry data, which indicate that CCL7 does not oligomerize on GAGs (26, 33, 35).

Introduction of an S8P Mutation in CCL7 Enhances Its Ability to Oligomerize on Heparin—One of the interesting sequence differences between CCL2 and CCL7 is the presence of a Ser at position 8, rather than a Pro as in all other MCPs (Fig. 1*A*). Because CCL2 and CCL8 form dimers in solution, and muta-

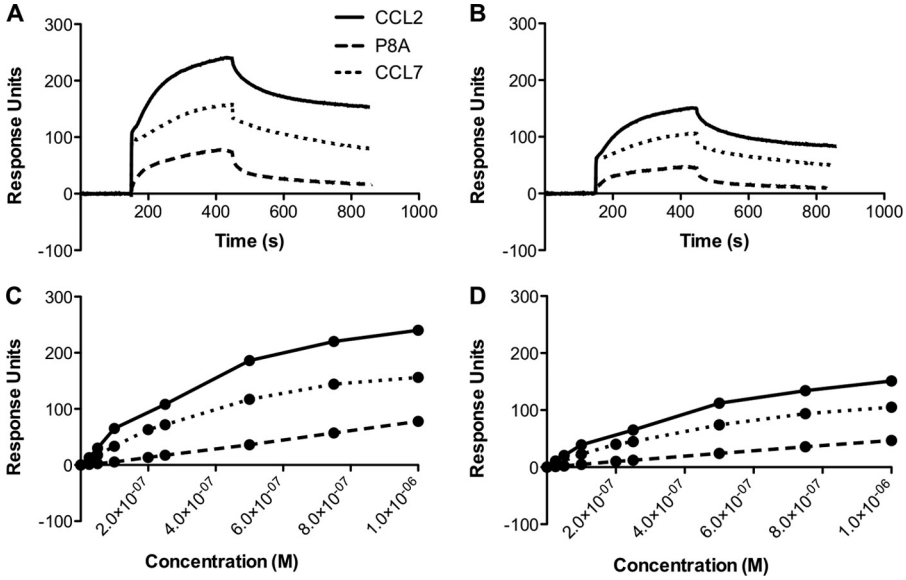

FIGURE 3. **CCL2(P8A) displays weaker interactions with GAG compared with CCL2 and CCL7.** SPR sensorgrams comparing CCL2 (*solid line*), CCL2(P8A) (*long dash*), and CCL7 (*short dash*) GAG interactions at the highest concentration tested (1 μM) show reduced binding of CCL2(P8A) relative to CCL2 and CCL7 on heparin (*A*) and HS (*B*) surfaces. Corresponding steady state curves of CCL2 (*solid line*), CCL2(P8A) (*long dash*), and CCL7 (*short dash*) at various concentrations (25–1000 nM) show accumulation of these chemokines on heparin (*C*) or HS (*D*) surfaces. Although accumulation of CCL7 is lower than CCL2 on both heparin and HS surfaces, the overall affinity is relatively unchanged (see Table 1).

tion of Pro at position 8 to Ala (P8A) in CCL2 impairs its ability to dimerize, we made a Ser-8 to Pro variant (S8P) of CCL7 with the expectation that it would oligomerize. Indeed, the cross-linking data of CCL7(S8P) looks similar to CCL2 and suggests that it has gained a propensity to oligomerize on GAGs (Fig. 2*A*). This result also further strengthens the conclusion that WT CCL7 is a natural non-oligomerizing chemokine, even in the presence of GAGs.

We also compared cross-linking results of CCL2, CCL2(P8A), CCL7, and CCL7(S8P) on HS (Fig. 2*B*). As expected, CCL7 remained mostly monomeric, similar to the CCL2 monomeric variant, CCL2(P8A) (Fig. 2*B*). However, in contrast to its oligomerization behavior in the presence of heparin octasaccharide, CCL2 did not form higher order oligomers, but remained mostly dimeric in the presence of HS (Fig. 2*B*). Similarly, CCL7(S8P) remained a dimer in the presence of HS (Fig. 2*B*). This data demonstrates that the type of GAG, and in particular, the differences in the extent of sulfation, can alter the structure/oligomerization state of a chemokine.

CCL2 and CCL7 Have a Higher Affinity for Heparin and HS Than the Non-oligomerizing CCL2(P8A) Variant—Because CCL7 does not oligomerize on GAGs, we were interested in comparing the affinities of CCL7 and CCL2 for heparin and HS, as well as the effect of oligomerization on the affinity of CCL2 for these GAGs, using the CCL2(P8A) mutant for comparison. SPR was used to obtain kinetic information about the chemokine-GAG interactions. In this setup, different concentrations of chemokine were passed over the surface of a C1 chip (no dextran matrix) coated with heparin or HS, and association (k_{on}) and dissociation (k_{off}) rates were determined to calculate overall affinity ($K_d = k_{off}/k_{on}$). As shown in Fig. 3, *A* and *B*, and Table 1, the affinity of CCL7 is within a factor of 2 of CCL2 for heparin (100 and 44 nM, respectively) and HS (120 and 70 nM, respectively). Despite their similar affinities, the amount of CCL7 that accumulated on the GAG was reduced relative to CCL2, presumably because of its inability to oligomerize (Fig. 3, *C* and *D*). Interestingly, however, the affinity of CCL7 for these surfaces of heparin and HS was ~5-fold higher than that of CCL2(P8A) (100 *versus* 570 nM for heparin; 120 *versus* 560 nM for HS) (Fig. 3, *A* and *B*, Table 1), consistent with the idea that oligomerization is important for the interaction of CCL2 with GAGs, whereas CCL7 can bind GAGs efficiently as a monomer. Accordingly, CCL7 exhibited greater accumulation on both heparin and HS surfaces compared with CCL2(P8A) (Fig. 3, *C* and *D*).

We also compared the ability of WT CCL7 and the S8P variant to bind to HS (Fig. 4, *A* and *B*). As predicted, more CCL7(S8P) accumulated on HS compared with WT CCL7 due to the ability of the mutant to oligomerize, similar to the greater accumulation of WT CCL2 compared with CCL2(P8A). On the other hand, the apparent affinities of WT *versus* mutant are similar (49 nM, Fig. 4*A*) in contrast to WT CCL2 and CCL2(P8A), which may be rationalized by a masking of CCL7 GAG-binding epitopes in the context of the dimer.

Identification of the Approximate GAG-binding Epitopes of CCL7 by Hydroxyl Radical Footprinting—Having established that CCL7 does not oligomerize on GAGs yet it still binds heparin and HS with affinities comparable with CCL2, we next set out to define the GAG-binding epitopes of CCL7. Previously, Ali and co-workers (7) targeted a B*X*B*XX*B motif (where B is a basic residue) in the 40s loop of CCL7 and subsequently designed a GAG-binding deficient variant of CCL7 that was significantly impaired in its ability to recruit cells *in vivo*. However, based on our previous characterization of the GAG-binding site of CCL2 and the high sequence homology of CCL2 and CCL7 (Fig. 1*A*), we hypothesized that the B*X*B*XX*B motif was not the sole contributor to the GAG-binding properties of CCL7 and that additional epitopes were likely responsible for

TABLE 1

Surface plasmon resonance analysis of the interaction of CCL2, CCL7, and mutants with heparin and "high density" HS

The rate of association (k_{on}) and the rate of dissociation (k_{off}) were used to calculate the equilibrium constant (K_d) where $k_{off}/k_{on} = K_d$. χ^2 values are provided as a measurement of the quality of the fit between the experimentally derived data and data from binding models as described under "Experimental Procedures."

	Heparin				HS (high density)			
	k_{on}	k_{off}	K_d	χ^2	k_{on}	k_{off}	K_d	χ^2
	$M^{-1}\,s^{-1}$	s^{-1}	M		$M^{-1}\,s^{-1}$	s^{-1}	M	
CCL2 WT	1.7×10^4	7.4×10^{-4}	4.4×10^{-8}	29.4	1.5×10^4	1.0×10^{-3}	7.0×10^{-8}	9.2
R18A/K19A			NOI[a]				NOI	
P8A	6.7×10^3	3.8×10^{-3}	5.7×10^{-7}	4.3	7.4×10^3	4.1×10^{-3}	5.6×10^{-7}	1.7
CCL7 WT	8.9×10^3	9.0×10^{-4}	1.0×10^{-7}	20.3	7.8×10^3	9.3×10^{-4}	1.2×10^{-7}	6.9
K18A/K19A	4.0×10^3	3.3×10^{-3}	8.3×10^{-7}	0.6	6.4×10^3	3.2×10^{-3}	5.0×10^{-7}	0.4
R14A/K18A/K19A	1.3×10^2	2.5×10^{-3}	1.9×10^{-5}	0.3	8.8×10^2	3.3×10^{-3}	3.7×10^{-4}	0.1
K18A/K19A/K22A			NOI				NOI	
K18A/K19A/R24A			NOI				NOI	
K44A/K46A/K49A	2.3×10^3	1.6×10^{-3}	6.8×10^{-7}	0.7	3.2×10^3	1.6×10^{-3}	5.1×10^{-7}	0.4
K69A/K70A	5.2×10^3	1.3×10^{-3}	2.5×10^{-7}	2.3	6.5×10^3	1.3×10^{-3}	2.1×10^{-7}	1.0
K65A/K69A/K70A/K75A	4.8×10^3	1.3×10^{-3}	2.8×10^{-7}	3.8	4.7×10^3	1.4×10^{-3}	3.1×10^{-7}	0.9

[a] NOI, no observable interaction.

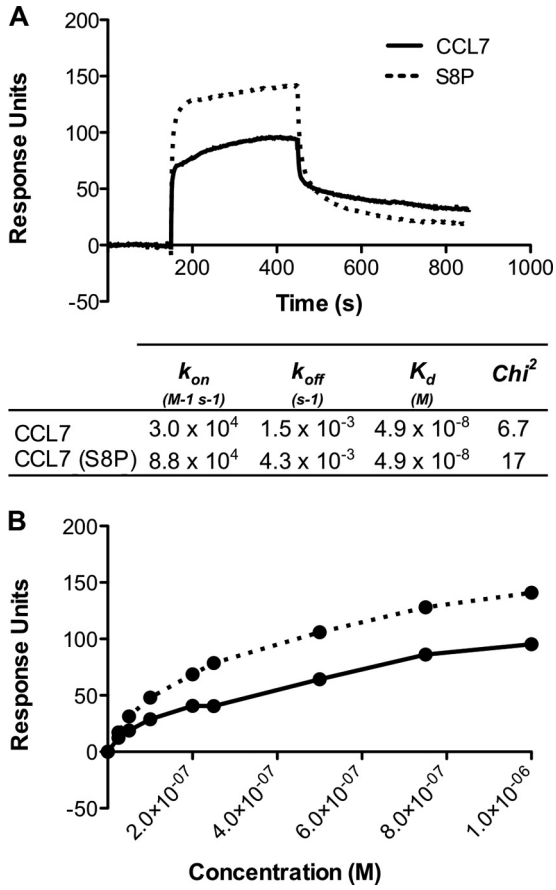

FIGURE 4. **The S8P mutation of CCL7 enhances accumulation on HS, whereas affinity is unchanged.** *A,* SPR sensorgram comparing 1 μM CCL7 (*solid line*) and CCL7(S8P) (*short dash*) on a HS surface and accompanying kinetic analysis from a concentration series ranging from 25 to 1000 nM. *B,* corresponding steady state curves of CCL7 (*solid line*) and CCL7(S8P) (*short dash*) at various concentrations (25–1000 nM) on a HS surface show enhanced accumulation of CCL(S8P) compared with CCL7.

its ability to function as a monomeric chemokine. In our previous study of CCL2, 35 mutants targeting primarily surface-exposed Lys and Arg residues were generated and characterized (11). To avoid such an extensive mutational undertaking with CCL7, we employed a novel method involving radiolytic footprinting coupled with mass spectrometry to localize regions of the chemokine protected by GAG. In this method, exposure to synchrotron x-ray radiation causes protein side chains to react with hydroxyl radicals formed from bulk solvent radiolysis, resulting in well defined oxidative modifications of the side chains (31). The modifications are then identified by proteolysis of the protein followed by mass spectrometry analysis of the peptides. Because the modification rate of side chains is proportional to the side chain solvent accessibility, a comparison of the modification rate in the presence and absence of GAG should reveal the footprint of the GAG on CCL7 due to protection from solvent (29, 36).

From these analyses (see "Experimental Procedures" for details), six peptides, corresponding to 72% sequence coverage were detected, whereas five peptides (63% sequence coverage) were identified in at least two experiments from samples of both CCL7 alone and CCL7 in complex with heparin octasaccharide, allowing for comparison of their oxidation rates (Table 2). Fig. 5 shows representative MS/MS spectra of modified and unmodified peptide-(13–27) and Fig. 6*A* shows representative dose-response curves for peptide-(13–27), in which there is an ~2-fold decrease in the oxidation rate in the presence of GAG. Residues Tyr-13, Arg-14, Phe-15, Lys-18, Ile-20, Pro-21, and Lys-22 from peptide-(13–27) (^{13}YRFINKKIPKQRLES^{27}), located in the so-called "N-loop," exhibited significant decreases in modification rate when GAG was present (Table 2). These data suggest a potential role for basic residues within this peptide in GAG-binding interactions. Given that the residues typically involved in GAG binding are Arg, Lys, and His, we first mapped the basic residues within the peptide sequence onto the structure of CCL7, to determine their solvent accessibility and likelihood of being true epitopes. Residues Lys-18, Lys-19, and Arg-24 seemed particularly well suited for GAG-binding, considering their solvent exposure (159.8, 176.7, and 123.9 Å^2, respectively) and their importance in the GAG interactions of CCL2 (Fig. 1, *A* and *B*) (11). Residues Arg-14 and Lys-22 in peptide-(13–27) were also attractive candidates, with solvent accessible surface areas of 178.1 and 103.4 Å^2, and a lack of conservation in CCL2 (Fig. 1*A*). A mutational study of these residues was therefore conducted to validate their importance in GAG interactions, as described below.

The C-terminal peptide-(63–76) (^{63}FMKHLDKKTQTPKL^{76}) along the C-terminal tail, specifically residues Met-64, His-66, Leu-67, Lys-69, and Lys-70, also showed a 2-fold decreased rate

TABLE 2

Modified peptides identified by mass spectrometry following radiolytic oxidation in the presence and absence of heparin octasaccharide

Bold amino acids indicate the amino acids modified by radiolytic oxidation. Solvent accessible surface areas (SA) are calculated for the modified amino acid side chains. Rates of oxidation are reported for the peptides in the presence and absence of GAG.

Peptide	Sequence	Residues modified (SA)	Modification rate	
			No GAG	+GAG
			s^{-1}	
13–27	**YR*****FIN**K**K**I**PK**QRLES[a]	Tyr-13 (122.5 Å) Arg-14 (178.1 Å) Phe-15 (78.1 Å) Lys-18 (159.8 Å) Ile-20 (7.1 Å) Pro-21 (63.2 Å) Lys-22 (103.4 Å)	32.8 ± 2.9	16.2 ± 1.3
44–59	**K**T**KL**DKEI**C**ADPTQ**KW**	Lys-44 (60.2 Å) Lys-46 (118.5 Å) Leu-47 (101.7 Å) Cys-52 (10.9 Å) Lys-58 (152.3 Å) Trp-59 (55.8 Å)	21.8 ± 2.4	17.4 ± 1.9
44–62	KT**KL**DKEI**C**ADPTQ**KW**VQD	Lys-46 (118.5 Å) Leu-47 (101.7 Å) Cys-52 (10.9 Å) Lys-58 (152.3 Å) Trp-59 (55.8 Å)	33.9 ± 4.4	30.1 ± 3.8
51–62	ICADPTQ**KW**VQD	Lys-58 (152.3 Å) Trp-59 (55.8 Å)	16.5 ± 2.0	10.9 ± 1.0
63–76	F**M**KL**HL**D**KK**TQTPKL	Met-64 (8.5 Å) His-66 (94.6 Å) Leu-67 (3.9 Å) Lys-69 (124.9 Å) Lys-70 (162.8 Å)	69.4 ± 7.5	25.9 ± 1.4

[a] R*, the presence of the modified b2 fragment ion in the MS/MS spectra of peptide-(13–27) indicates that +16 Da modification can occur at either Tyr-13 or Arg-14. The elution time of this peptide from the reversed-phase C18 column that was observed to be 1 min later than elution time for its unmodified form suggests that modification may occur at Arg-14.

of oxidation in the presence of GAG compared with CCL7 alone (Fig. 6*B*). Residues in this peptide could constitute a genuine binding site for GAGs, as it is rich in solvent-exposed Lys and His residues including Lys-65, His-66, Lys-69, Lys-70, and Lys-75 (Fig. 1, *A* and *B*), which have solvent accessibilities of 140.4, 94.6, 124.9, 162.8, and 147.1 $Å^2$, respectively. Furthermore, the distance and orientation of this epitope relative to epitopes in peptide-(13–27) suggests that together they could comprise a contiguous binding site.

In contrast to the above, peptide-(51–62) (^{51}ICADPTQKWVQD^{62}) revealed a much smaller decrease in oxidation rate, around 30% (Table 2). Lys-58 is the sole basic residue within this region, and, although highly solvent accessible, was found previously to have little effect on the binding of CCL2 to heparin (11), consistent with the modest changes observed here. Two peptides encompassing the known 40s loop B*X*B*XX*B motif were also oxidized by radiolytic footprinting, peptide-(44–59) (^{44}KTKLDKEICADPTQKW^{59}) and peptide-(44–62) (^{44}KTKLDKEICADPTQKWVQD^{62}). Although GAG-dependent decreases in modification of 10–20% were observed, they were not significant. However, similar to peptide-(51–62), a highly reactive Trp residue in each 40s loop peptide is likely dominating the oxidation signal. As the method used here averages the reactivity of ALL residues in a peptide, if the Lys residues are exhibiting changes, whereas the more reactive Trp residues are unaffected, the net result can be an overall inability to observe a significant change. Nevertheless, as previously demonstrated (7), and confirmed below, the 40s loop is a clear GAG-binding epitope of CCL7. Although a peptide encompassing residues 1–7 was observed, no modification was detected within this region in both ±GAG.

Heparin-Sepharose Characterization of CCL7 Mutants Confirms Two Previously Unidentified GAG-binding Epitopes—The hydroxyl radical footprinting data suggested a potential GAG-binding role of epitopes in peptide-(13–27) along the N-loop and the C terminus of CCL7, based on the reduced oxidation rate of these regions in the presence of excess GAG. To validate the contribution of these sites to GAG binding, we generated several Ala mutants and tested them in GAG-binding affinity assays. Two methods were used for validation: heparin-Sepharose chromatography and SPR. Heparin-Sepharose chromatography was used first as it is a fast, straightforward and commonly used method to rank the relative "affinity" of chemokines and mutants for GAGs. In this assay, the amount of salt needed for elution of chemokine from a heparin-Sepharose column, $\Delta[NaCl]_H$, was determined. WT and mutant CCL7 were therefore subjected to this assay and the results are summarized in Table 3. The $\Delta[NaCl]_H$ between mutant and WT is plotted in Fig. 7, where larger values suggest greater destabilization of the GAG interaction due to the mutation. WT CCL2, the non-oligomerizing mutant CCL2(P8A) and the previously identified GAG-binding deficient mutant, CCL2(R18A/K19A) (11), were used as controls for comparison to WT and mutant CCL7.

Similar to the CCL2(R18A/K19A) mutant, all of the chosen CCL7 GAG mutants displayed a decreased affinity for GAG (Table 3, Fig. 7). The K18A/K19A mutant of CCL7 exhibited a significant decrease in heparin binding, with a $\Delta[NaCl]_H$ of 179.3 mM. However, it was not as destabilized as the corresponding R18A/K19A mutant of CCL2, which showed a $\Delta[NaCl]_H$ of 300.3 mM. This finding can be rationalized by the fact that CCL2 oligomerizes on heparin, whereas CCL7 does not, and the effect of the mutation would therefore be magni-

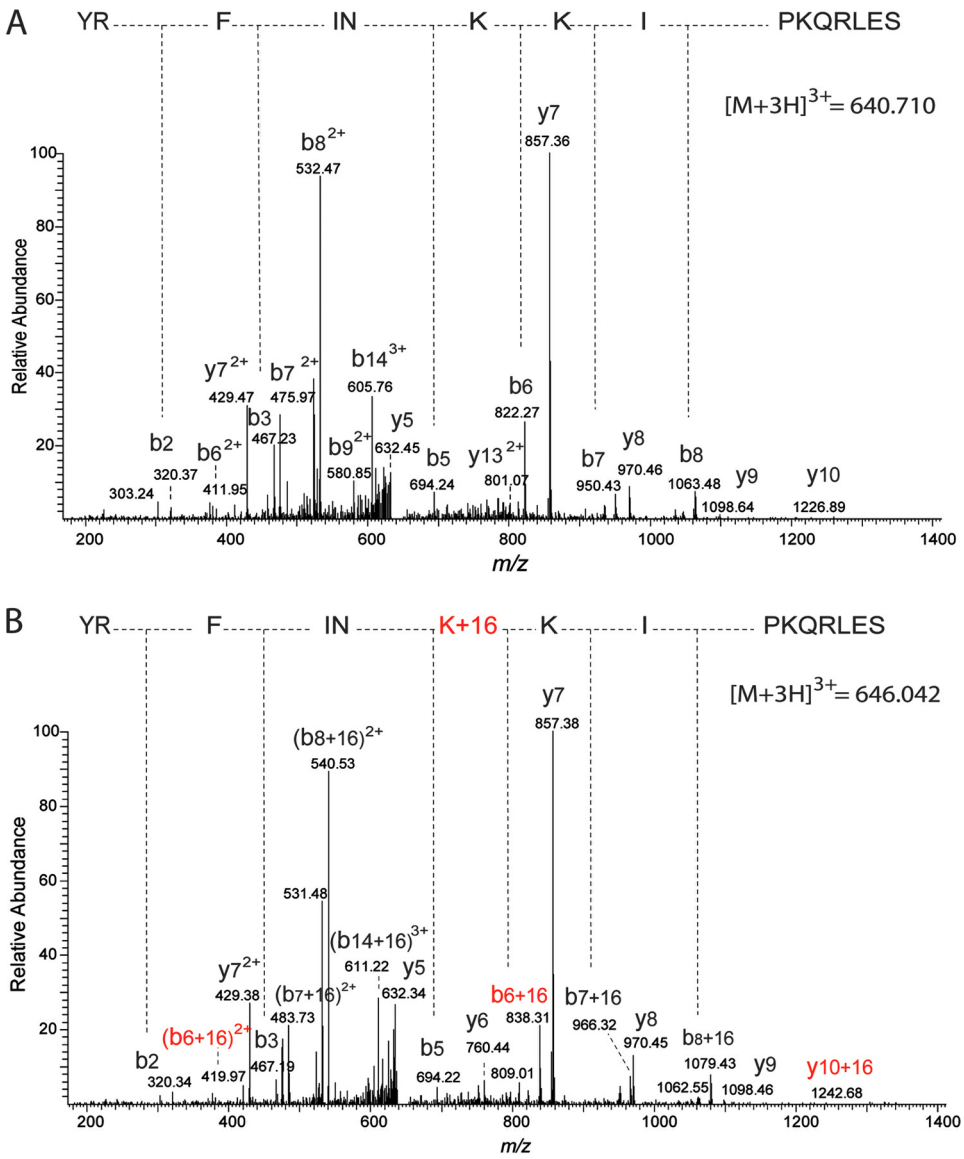

FIGURE 5. **MS/MS spectra of the unmodified (*A*) and modified (*B*) peptide-(13–27) ([13]YRFINKKIPKQRLES[27]) derived from pepsin digestion of CCL7 following irradiation for 10 ms.** The presence of the unmodified b_5 and y_9 ions, and modified b_6 and y_{10} ions (*B*) shows the modification of this peptide at Lys-18.

fied in the context of the oligomerizing chemokine. However, combining the K18A/K19A mutation of CCL7 with additional mutations within peptide-(13–27) (R14A, K22A, and R24A) further destabilized the CCL7 interaction; in particular, R24A, a residue also common to the GAG-binding site of CCL2 (11), had the most pronounced effect. It is also noteworthy that all of the double and triple mutations in this region had a more pronounced effect than the previously identified 40s loop CCL7 mutant (K44A/K46A/K49A) suggesting that the N-loop residues constitute the dominant GAG-binding epitope of CCL7. The C-terminal tail residues also affected heparin binding, with $\Delta[NaCl]_H$ values ranging from ~70 to 130 mM depending on the number of Ala mutations introduced. Each Ala mutation had an additive effect on heparin binding (data not shown) with the quadruple mutant (K65A/K69A/K70A/K75A) showing the greatest loss of affinity, and was therefore used for all subsequent analyses. CCL7(S8P) was also investigated to determine whether its apparent ability to oligomerize affected its affinity for heparin. Indeed, it showed an increased interaction relative to WT CCL7, indicated by a negative $\Delta[NaCl]_H$ value, in contrast to CCL2(P8A), which showed reduced heparin binding relative to WT CCL2 (Table 3, Fig. 7).

Measurements of $\Delta[NaCl]_H$ are sometimes done in parallel with measurements of the amount of salt required to elute WT *versus* mutant chemokine from a nonspecific SP-Sepharose column ($\Delta[NaCl]_S$), and the difference between these values is used to calculate $\Delta\Delta[NaCl]$. The $\Delta\Delta[NaCl]$ value is then interpreted as a measure of specificity of the protein-heparin interaction, with positive values indicating a specific interaction. $\Delta\Delta[NaCl]$ values are included in Table 3 for completeness; however, in our experience these numbers are not always reliable because of differences in variables such as the density of binding sites on the two resins. Nevertheless, $\Delta[NaCl]_S$ generally mirrors the $\Delta[NaCl]_H$, confirming the contribution of Arg-14, Lys-18, Lys-19, Lys-22, and Arg-24 in the N-loop and to a lesser degree, the C-terminal domain. These two regions have

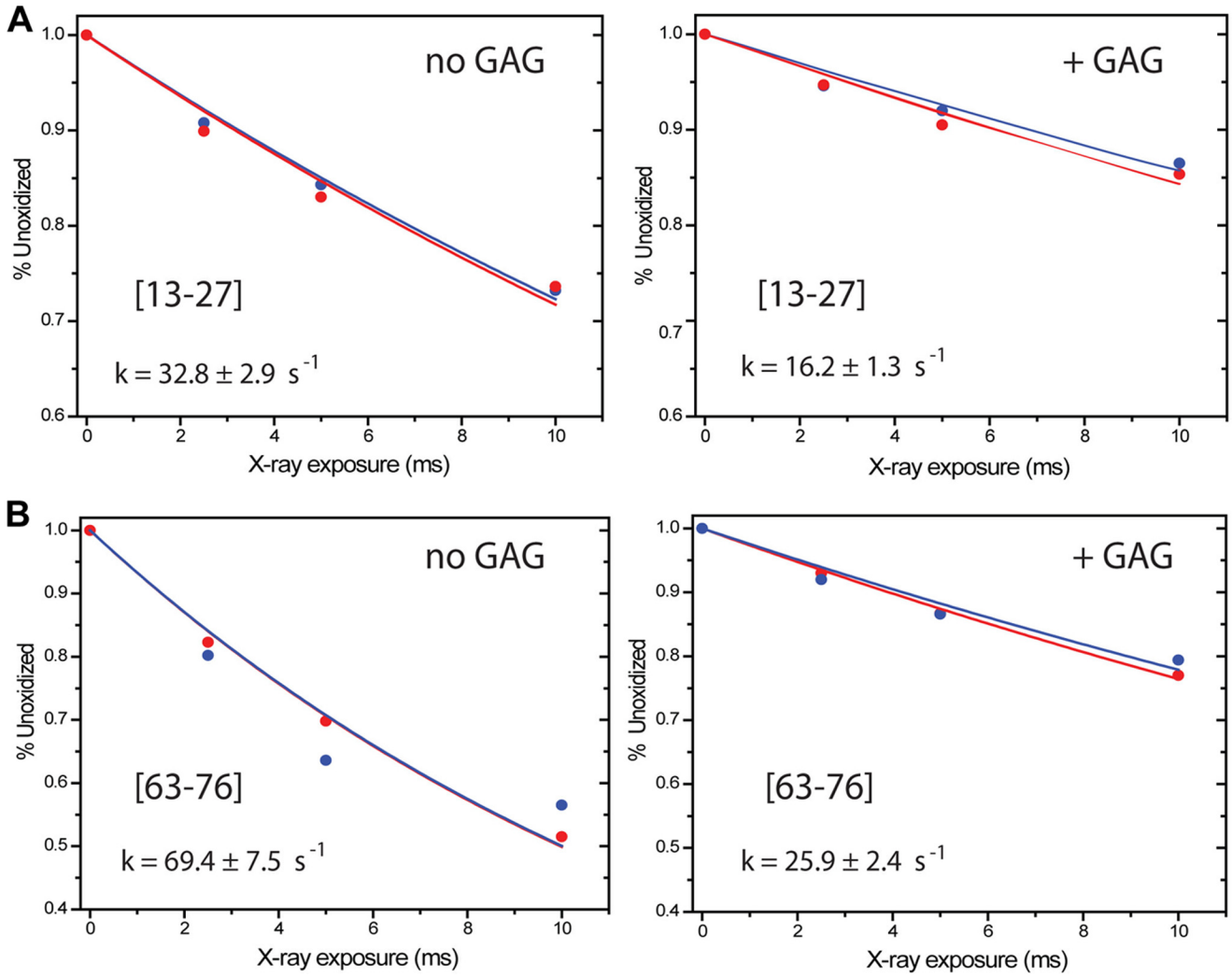

FIGURE 6. **Oxidation rates of peptide-(13–27) (*A*) and peptide-(63–76) (*B*) in the presence (*right*) and absence (*left*) of GAG.**

TABLE 3

Heparin-Sepharose affinity characterization of CCL7, CCL2, and mutants

The concentration of NaCl (mM) required to elute protein from a heparin or a SP-Sepharose affinity column is indicated as $[NaCl]_H$ and $[NaCl]_S$, respectively. $\Delta[NaCl]_H$ and $\Delta[NaCl]_S$ are the difference in $[NaCl]_H$ and $[NaCl]_S$ between WT and mutant protein, respectively. $\Delta\Delta[NaCl]$ is the specificity index where $\Delta\Delta[NaCl] = \Delta[NaCl]_H - \Delta[NaCl]_S$ as described under "Experimental Procedures."

WT and mutant proteins	$[NaCl]_H$	$\Delta[NaCl]_H$	$[NaCl]_S$	$\Delta[NaCl]_S$	$\Delta\Delta[NaCl]$
			mM		
CCL7 WT	666.0 ± 6.0	0.0 ± 8.5	612.7 ± 7.0	0.0 ± 9.9	0.0 ± 13.1
K18A/K19A	486.7 ± 5.0	179.3 ± 7.8	428.7 ± 3.1	184.0 ± 7.6	−4.7 ± 10.9
R14A/K18A/K19A	449.5 ± 2.8	216.5 ± 6.6	378.7 ± 2.3	234.0 ± 7.4	−17.5 ± 9.9
K18A/K19A/K22A	428.7 ± 4.2	237.3 ± 7.3	368.7 ± 3.1	244.0 ± 7.6	−6.7 ± 10.6
K18A/K19A/R24A	413.0 ± 1.0	253.0 ± 6.1	358.7 ± 2.3	254.0 ± 7.4	−1.0 ± 9.6
K44A/K46A/K49A[a]	582.0 ± 2.0	146.0 ± 8.9	504.0 ± 0.0	136.7 ± 1.2	9.3 ± 9.0
K65A/K69A/K70A/K75A[a]	598.0 ± 2.0	130.0 ± 8.9	533.0 ± 12.7	107.7 ± 12.8	22.3 ± 16.0
S8P	820.0 ± 0.0	−154.0 ± 6.0	692.7 ± 5.8	−80.0 ± 9.1	−74.0 ± 10.9
CCL2 WT	687.3 ± 9.2	0.0 ± 13.0	523.3 ± 1.2	0.0 ± 1.7	0.0 ± 13.1
R18A/K19A[b]	446.7 ± 4.6	300.3 ± 8.4	331.0 ± 1.4	261.0 ± 3.1	39.3 ± 9.0
P8A	550.0 ± 0.0	137.3 ± 9.2	466.7 ± 4.2	56.6 ± 4.3	80.7 ± 10.2

[a] Mutant profiled separately. For comparison, CCL7 WT $[NaCl]_H$ = 728.0 ± 8.7 mM and CCL7 WT $[NaCl]_S$ = 640.7 ± 1.2 mM.
[b] Mutant profiled separately. For comparison, CCL2 WT $[NaCl]_H$ = 747.0 ± 7.0 mM and CCL2 WT $[NaCl]_S$ = 592.0 ± 2.8 mM.

not been previously associated with CCL7-GAG interactions, and therefore represent new GAG recognition sites in addition to the 40s loop motif.

Surface Plasmon Resonance Validation of the CCL7 Mutants Suggest That CCL7 Has a More Dense GAG-binding Epitope in the Context of the Monomer Than CCL2—Heparin-Sepharose chromatography provides a rapid way to identify potential GAG-binding epitopes. However, it is not a true measure of affinity and commercial sources of resin only contain immobilized heparin. Therefore, as a second validation approach, we used SPR and investigated interactions of the chemokines/mutants with heparin and HS-coated SPR chips. Fig. 8, *A* and *B*, and Table 1 show a comparison of WT CCL7 with mutants corresponding to the three GAG recognition sites (the N-loop,

the 40s loop, and the C terminus). Notably, all of the analyses were performed at the same time and on the same chip, and the trends were consistent with similar analyses performed on another chip as well. As expected from the heparin-Sepharose chromatography results, the CCL7(K18A/K19A) mutant had a significantly lower affinity for both heparin and HS compared with WT CCL7 (830 *versus* 100 nM for heparin and 500 *versus* 120 nM for HS), and also showed a slightly lower heparin affinity compared with the 40s loop mutant (680 nM). However, the K18A/K19A CCL7 mutation did not completely eliminate binding to heparin or HS like the corresponding R18A/K19A mutation in CCL2 (Fig. 8, *C* and *D*, and Table 1). These differences may be explained by the generally stronger interaction of Arg compared with Lys in GAG binding (37) as well as differences in oligomerization, as discussed above. The inclusion of R14A as a triple mutant of CCL7 reduced the affinity further, and the triple mutants including K22A and R24A showed no interaction with heparin or HS. The C-terminal quadruple mutant (K65A/K69A/K70A/K75A) had the least impact on binding affinity, and the reduction was mostly due to a slower on-rate, which might be expected given the flexibility of the C terminus of CCL7. Remarkably, all of these data are consistent with the heparin-Sepharose chromatography results. In Fig. 1, *A* and *B*, the GAG-binding epitopes are highlighted on the sequence alignment and on the monomeric structures of CCL7 and CCL2 for comparison. Although it is clear that CCL7 and CCL2 share common residues that contribute to GAG binding, the number of residues that contribute to GAG interactions is higher in CCL7 than in CCL2, consistent with the ability of CCL7 to bind GAGs with sufficiently high affinity as a monomer.

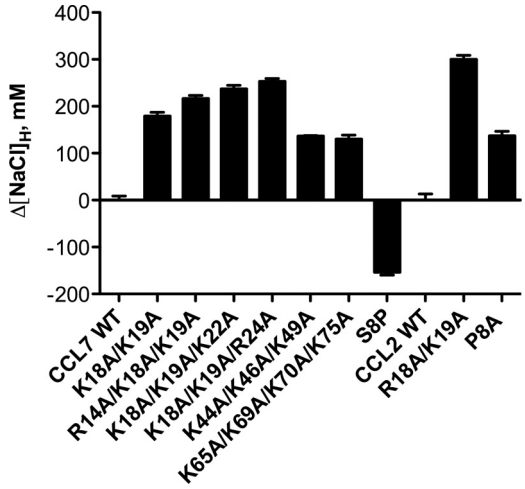

FIGURE 7. **Heparin-Sepharose chromatography results for CCL7, CCL2, and select mutants.** The difference in the concentration of NaCl (mM) required to elute mutant chemokine from heparin-Sepharose compared with WT chemokine is plotted as the average of three experiments (± S.D.).

Monomeric CCL2(P8A) and CCL7 Are More Sensitive Than CCL2 to the Density of HS Coated on the SPR Chip Surfaces—In the course of the SPR studies, we observed that the density of HS immobilized on the SPR chips had a significant effect on the observed interaction kinetics of some chemokines. As described above, CCL2(P8A) showed an affinity of 570 and 560 nM on heparin and high density HS, respectively (Table 1). However, when examined on a chip with lower density HS, the affinity dropped ~100-fold, to 52.6 (medium density HS) and 64.7 μM (low density HS) (Table 4), in stark contrast to WT CCL2 where affinities were relatively similar across all HS densities tested (70, 84, and 139 nM for high (Table 1), medium, and low (Table 4) HS, respectively). Similarly, the affinity of CCL7

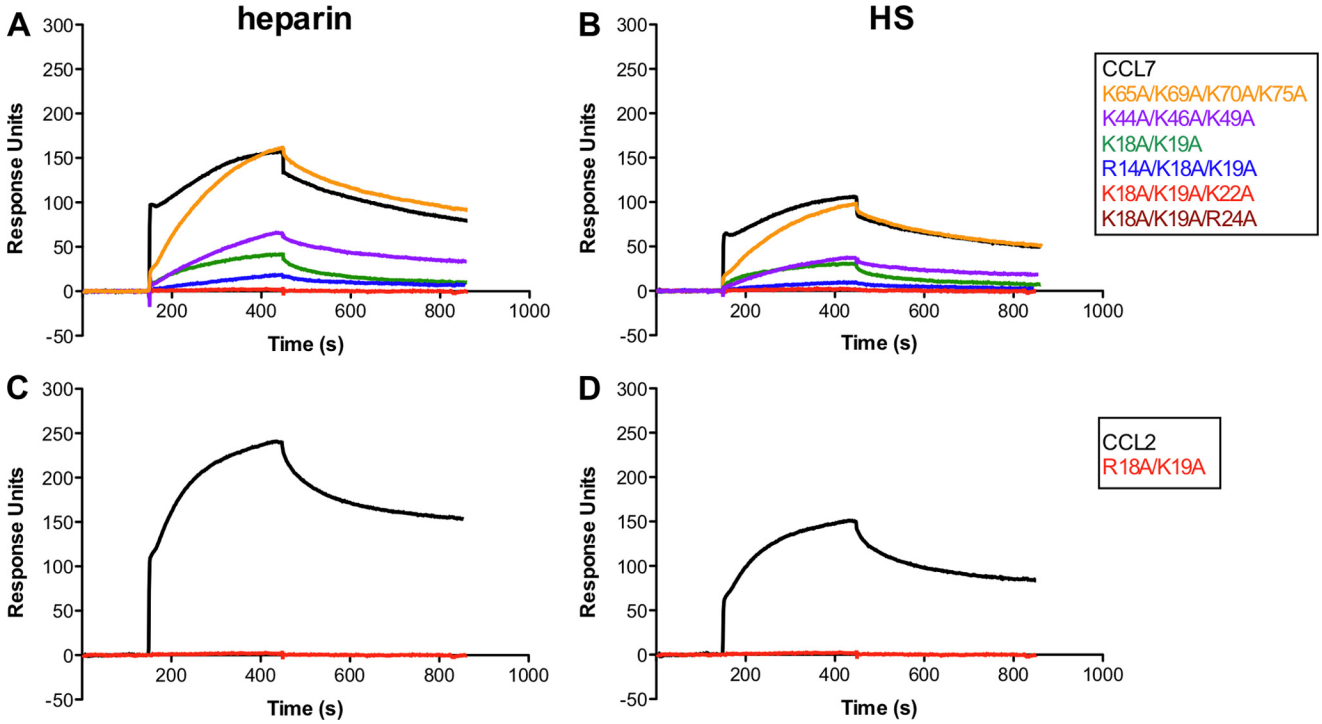

FIGURE 8. **Characterization of CCL7 and CCL2 GAG mutants by SPR analysis.** SPR sensorgrams comparing CCL7 and mutants at 1 μM over heparin (*A*) and HS (*B*) surfaces and CCL2 and CCL2(R18A/K19A) GAG mutant over heparin (*C*) and HS (*D*) surfaces.

TABLE 4
Density dependence of CCL2, CCL2(P8A) and CCL7 for medium and low density HS (compared to high density HS, Table 1)

	HS (medium density)				HS (low density)			
	k_{on}	k_{off}	K_d	χ^2	k_{on}	k_{off}	K_d	χ^2
	$M^{-1}\,s^{-1}$	s^{-1}	M		$M^{-1}\,s^{-1}$	s^{-1}	M	
CCL2	1.44×10^{4}	1.21×10^{-3}	8.40×10^{-8}	13.10	1.24×10^{4}	1.72×10^{-3}	1.39×10^{-7}	2.82
CCL2(P8A)	6.80×10^{1}	3.58×10^{-3}	5.26×10^{-5}	5.30	3.00×10^{2}	1.94×10^{-2}	6.47×10^{-5}	0.61
CCL7	8.83×10^{3}	6.81×10^{-3}	7.71×10^{-7}	1.83	6.37×10^{2}	1.54×10^{-2}	2.42×10^{-5}	1.70

was decreased on the medium and low density HS surfaces (771 nM and 24.2 μM, respectively, Table 4) compared with high density HS (120 nM, Table 1) although these differences were not as exaggerated as the monomeric variant CCL2(P8A), presumably due to the more extensive GAG-binding surface within the monomeric structure of CCL7 compared with CCL2(P8A). Notably, the chemokine concentration required for obtaining a sufficient signal for kinetic analysis of CCL2(P8A) on the medium and low density HS surfaces was 3-fold higher than that used for CCL7 and CCL2 (Table 4), further underscoring the importance of oligomerization for high affinity GAG binding of CCL2. Our interpretation of these data is that CCL2 requires oligomerization to bridge multiple sulfation sites either within or between GAG chains for high affinity binding. In the case of CCL7, multiple GAG epitopes help it to partially compensate for its lack of oligomerization relative to CCL2(P8A); nevertheless, the dependence of its affinity on GAG chain density also suggests that it requires bridging sulfation sites on separate GAG chains.

Interaction of CCL2, CCL7, and Mutants on Endothelial Cells Is Consistent with GAG-binding Affinities Determined by SPR and Heparin-Sepharose Chromatography—To confirm the biological relevance of the newly identified N-loop GAG-binding epitopes of CCL7, and how they compare with CCL2 and mutants, we investigated the ability of CCL2, CCL7, and the GAG and oligomerization mutants to bind GAGs on the EA926 endothelial cell line. Fig. 9*A* shows detection of CCL2, CCL2(P8A), and CCL2(R18A/K19A) on EA926 cells with an anti-CCL2 antibody. Consistent with the heparin-Sepharose chromatography and the SPR results, CCL2(P8A) and CCL2(R18A/K19A) show significantly reduced accumulation on these cells in comparison to WT CCL2. Fig. 9*B* shows results for CCL7 and the various CCL7 GAG mutants. Again, the results mirror the chromatography and SPR results with the CCL7(K18A/K19A/K22A) and CCL7(K18A/K19A/R24A) mutants showing the least ability to bind to the EA296 cells. Although difficult to compare directly due to the employment of different antibodies, the data seem to indicate that the CCL7(K18A/K19A) mutant shows a greater ability to bind to the cells compared with the CCL2(R18A/K19A) mutant, in accordance with the SPR data, and binds slightly less well than the CCL7 40s loop mutant.

CCL7(K18A/K19A) Is Capable of Promoting Cell Migration in Vitro—We also examined the ability of specific chemokine mutants to promote transendothelial cell migration as a measure of their ability to activate receptor. As expected, CCL2(P8A) promotes migration of monocytes as efficiently as WT CCL2, whereas CCL2(R18A/K19A) exhibits an ~10-fold shift in potency, likely due to a slight overlap of the GAG and receptor binding epitopes, as demonstrated previously (5) (Fig. 10*A*). The analogous mutant of CCL7, CCL7(K18A/K19A), is also capable of promoting monocyte migration with only a slight decrease in potency compared with WT CCL7 (Fig. 10*B*). Similar to CCL2, the results suggest a slight overlap between the GAG and receptor binding epitopes on CCL7 because if the reduced potency was due to the need for GAG-mediated presentation for receptor activation (38) one would expect a more pronounced effect.

DISCUSSION

A key question that we set out to address in this study is why CCL7 is able to promote robust migration *in vivo*, despite its lack of oligomerization, whereas many other chemokines require oligomerization for their *in vivo* function? This issue is related to the broader question as to why there is such a diverse range of oligomerization states, with some chemokines forming monomers in solution, others forming dimers and tetramers with varying ranges of stability, and still others forming polymers. Oligomerization is thought to be important, minimally for binding to GAGs, and indeed, chemokine interactions with GAGs can stabilize oligomers (26), or promote oligomerization of weakly associating chemokines (39, 40). For example, SDF-1/CXCL12 has a very weak propensity to dimerize in solution with an affinity constant ranging from micromolar to millimolar depending on the buffer conditions (39). However, the dimer is stabilized by GAGs, dimerization increases its affinity for GAGs *in vitro* (13) and it avidly binds to GAGs on cell surfaces (41). In this study, we showed that CCL7 does not oligomerize on GAGs in solution, consistent with prior studies done by mass spectrometry in the gas phase, and in stark contrast to other members of the MCP family. We therefore hypothesized that CCL7 must have higher affinity for GAGs as a monomer compared with monomeric subunits of other oligomerizing chemokines, and in particular, the highly related chemokine, CCL2. Fortunately, many years ago, a non-oligomerizing variant of CCL2 (CCL2(P8A)) was identified (9) and its GAG-binding epitopes characterized in our laboratory (11), which could be used in direct comparison to the GAG-binding epitopes of CCL7.

Traditional methods for identifying GAG-binding sites of chemokines have typically involved mutagenesis of the chemokine (mainly Arg, Lys, and sometimes His residues), followed by characterization of the ability of the mutants to bind to GAGs (generally heparin). Approaches to assess GAG binding include isothermal fluorescence titration (42, 43), heparin affinity chromatography (11, 16, 18), filter-based GAG-binding assays (43, 44), SPR (13, 45), and ^{1}H-^{15}N HSQC NMR chemical shift perturbation experiments (13, 18, 46). These experiments generally require cloning, expression, and purification of many

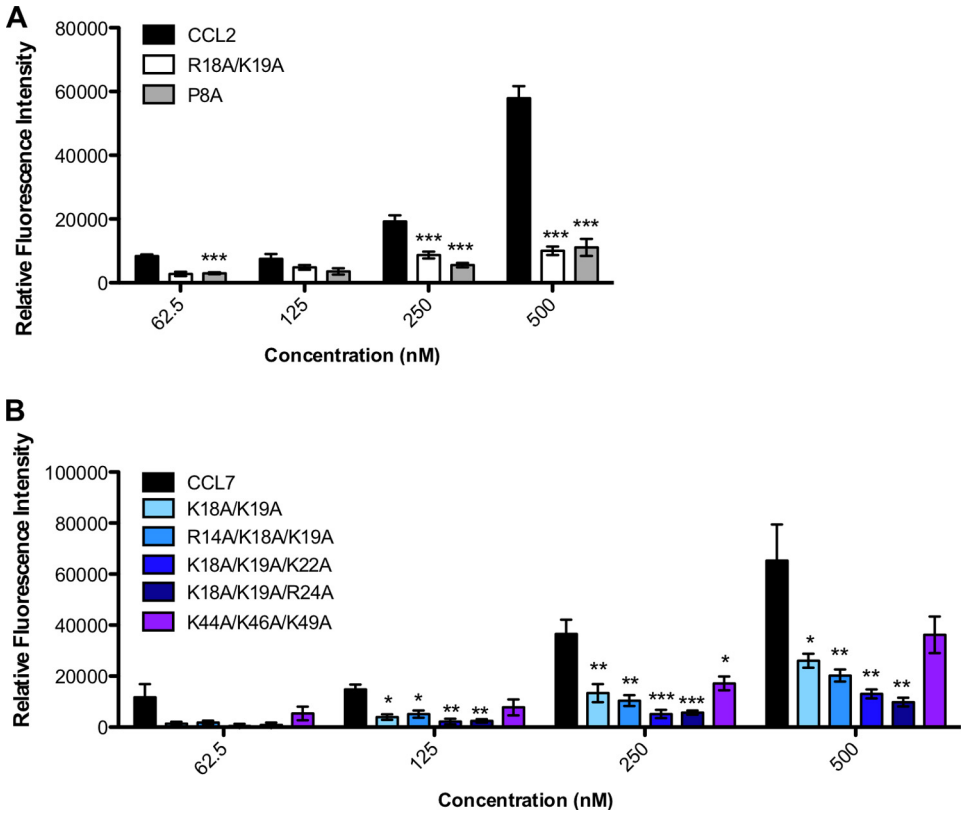

FIGURE 9. **Detection of surface bound CCL2, CCL7, and GAG mutants on the EA926 endothelial cell line.** Chemokine was incubated on EA926 cells at specified concentrations and then detected by either an anti-CCL2 (*A*) or anti-CCL7 antibody (*B*). Quantification of the relative fluorescence intensity of WT or mutant chemokine at varying concentrations is shown as the average of three independent experiments performed in at least duplicate (mean ± S.E.). Statistical significance was determined using a one-way analysis of variance (Bonferroni post test) and indicated values are as follows: *, $p < 0.05$; **, $p < 0.01$; ***, $p < 0.001$.

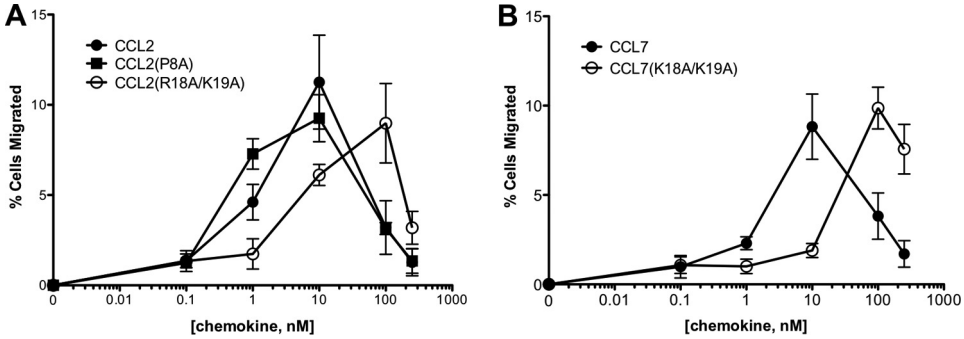

FIGURE 10. ***In vitro* transendothelial migration of monocytes toward varying concentrations of CCL2, CCL2(P8A), and CCL2(R18A/K19A) (*A*) and CCL7 and CCL7(K18A/K19A) (*B*).** Shown are data averaged from three independent experiments performed in at least duplicate (mean ± S.E.).

mutants to assess the contribution of specific residues to GAG binding. For example, in the work by Lau *et al.* (11) an extensive analysis of 35 mutants of CCL2 was conducted. On the other hand, many other studies have characterized significantly fewer mutants, targeting single GAG motifs (*e.g.* BB*X*B and B*X*B*XX*B), which has resulted in the identification of GAG binding-deficient chemokines that are extremely useful for functional studies, but provide incomplete characterization of the GAG-binding surface of the chemokine for the purpose of understanding GAG recognition and specificity. As an alternative method for the unbiased identification of GAG-binding sites of CCL7 that limits the number of mutants that need to be made and subsequently characterized, we used hydroxyl radical footprinting. Hydroxyl radical footprinting is a mass spectrometry based technique that has been successfully used to characterize protein complexes (31, 47, 48), but to our knowledge, this is the first report where it has been used to characterize protein complexes with GAGs. The essence of the technique is that interactions of proteins with other molecules, which result in reduced solvent accessibility to modification by reactive hydroxyl radicals, can be used to footprint the interaction sites between the protein of interest and the interacting molecule. However, changes in oxidation can also be caused by ligand binding-induced conformational changes remote from the binding epitopes (allostery), and in the case of many chemokines, by protein oligomerization. However, because CCL7 does not oligomerize on GAGs, it is a good candidate for these studies and for evaluating the general utility of the method for

characterizing protein-GAG interactions. Using this method we identified two novel and topographically distinct potential GAG-binding sites of CCL7 in the N-loop and along the C-terminal tail. Confirming the contribution of specific residues within these regions to GAG binding required the generation and characterization of only seven new mutants.

The results from heparin-Sepharose affinity chromatography and SPR confirmed that CCL7 has two major epitopes involved in GAG binding: the previously reported 40s loop and the newly identified N-loop. The C terminus also seems to be involved but to a lesser degree. Lys-18 and Lys-19 were shown to be the most critical residues for interaction of CCL7 with GAGs, similar to the corresponding Arg-18 and Lys-19 mutations of CCL2, yet mutation of these residues in CCL7 does not abolish GAG binding in contrast to CCL2, where it does. This is not entirely surprising because it has been previously established that Arg bind GAGs tighter than Lys (37). An alternative explanation is that the more dense network of GAG-binding residues of CCL7 in this region may necessitate the mutation of more than two residues to completely block binding. Nevertheless, these data reinforce the concept that CCL7 binds to GAGs more strongly as a monomer than CCL2 and that these differences are likely due to a more concentrated (and perhaps effective) network of GAG-binding residues. This idea is also supported by the stronger affinity of CCL7 compared with CCL2(P8A) in binding both heparin and HS.

Interestingly, enhancing the ability of CCL7 to dimerize with an S8P mutation increased its accumulation on GAGs, but it did not increase its affinity according to SPR data. This suggests that CCL7 has evolved to overcome its lack of oligomerization by having a GAG-binding surface self-contained within the monomer that suffices for high affinity interactions with GAGs. Modest but important sequence differences can partially explain the results (Fig. 1*A*): the following residues that contribute to GAG binding in CCL7, listed first, would not be predicted to contribute substantially to GAG-binding in CCL2, listed second in parentheses: Arg-14(Asn-14), Lys-22(Val-22), Lys-46(Ile-46), and Lys-70(Gln-70), as Arg and Lys are dominant residues in GAG binding (37). In addition to the major N-loop epitope identified herein, heparin affinity chromatography and SPR data also point to a minor role of the C terminus in GAG binding. Mutation of basic residues along this region (Fig. 1, *A* and *B*) result in a modest decrease in binding to heparin-Sepharose beads and ~2–3-fold reduction in heparin and HS affinity according to SPR. However, these residues likely comprise a secondary recognition site, unlike the C-terminal domains of other chemokines, like CXCL8 and CXCL12-γ, which are thought to strongly contribute to GAG interactions (17, 49). Instead, for CCL7, the C terminus may help facilitate proper orientation or stabilization of more important GAG recognition sites through nonspecific electrostatic interactions, similar to what has been reported for the D2 cationic domain of IFNγ (50).

Previously, Ali and co-workers (7) showed that the 40s loop CCL7 mutant (K44A/K46A/K49A), not only did not recruit cells *in vitro*, but also did not promote chemokine-induced inflammation and effectively blocked WT activity in an air pouch mouse model. The mechanism was attributed to the inability of the GAG mutant to localize on cell surfaces, while maintaining an ability to activate receptor, resulting in systemic receptor desensitization. Moreover, this group demonstrated not only homologous desensitization, but also heterologous desensitization mediated by GAG mutants in an air pouch model (7). The newly identified CCL7(K18A/K19A) mutant reported in this study may also be useful in blocking inflammation as it has only a small effect on receptor activation, which is likely due to a slight overlap between the receptor and GAG-binding sites of the chemokine, similar to CCL2(R18A/K19A). Consequently, CCL7(K18A/K19A) should still promote receptor desensitization, but because it binds GAGs more weakly than the 40s loop mutant, it could potentially have as much and possibly more anti-inflammatory activity. On the other hand, tissue-specific differences have been observed and in fact when instilled in the lung, GAG-deficient mutants of CXCL8 actually caused enhanced accumulation of neutrophils, which likely reflects the effects of tissue structure and GAG composition on the formation of chemokine gradients (32, 51).

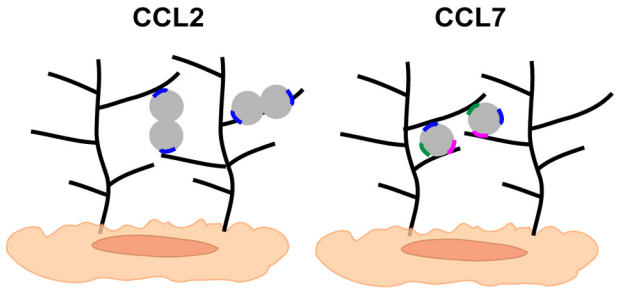

FIGURE 11. **Model of GAG interactions mediated by CCL2 and CCL7.** SPR analysis of the effects of variable density HS on chemokine-GAG interactions reveals the sensitivity of CCL7 to low HS levels compared with oligomerization-prone WT CCL2, which is much less sensitive. This data suggests that CCL2, which can form dimers in the presence of HS (Fig. 2*B*), may be able to bind to single GAG chains or bridge separate GAG chains to achieve high affinity binding through its GAG epitope (depicted in *blue*) located on opposing sides of the dimer structure (*left*). By contrast, CCL7 has multiple GAG recognition sites (depicted as *blue*, *green*, and *magenta*, *right*) that confer a similar affinity as CCL2 for high density GAGs by bridging multiple GAG chains, but the inability of CCL7 to oligomerize causes reduced affinity when the GAG chain density is low. That the lack of CCL7 oligomerization is responsible for its lower affinity for low density GAG surfaces compared with CCL2 is supported by the fact that monomeric CCL2(P8A) shows an even greater decrease in affinity on the low density *versus* high density HS surfaces than CCL7.

Although this work was focused primarily on CCL7, the comparative studies of CCL2 revealed new information about this chemokine as well. One serendipitous observation made in this study is that CCL2(P8A) has a significantly lower affinity for HS when it is immobilized at low density compared with when it is immobilized at a comparatively higher density, in contrast to WT CCL2. Interestingly, the interaction of CCL7 also showed a dependence on density, although it was not as striking as CCL2(P8A). This suggests that different epitopes on the chemokines can bridge GAG chains to achieve high affinity binding as illustrated in Fig. 11. However, because the affinity of CCL2(P8A) is lower than CCL7 and significantly lower than WT CCL2, due to its lack of oligomerization, it shows the greatest sensitivity to the GAG density. In contrast, and whereas preliminary, the dependence of affinity on heparin density appears to be less pronounced than with HS (data not shown), suggesting that the high abundance of sulfate groups along a

given heparin chain may alleviate the need for chemokines to bridge GAG chains. Additionally and although entirely speculative, the sensitivity of chemokine binding to GAGs on the density of GAG chains could provide a mechanism for regulating chemokine localization and function *in vivo*.

These findings may also help to explain previously observed anti-inflammatory activities of CCL2(P8A). This monomeric chemokine variant is fully capable of activating CCR2 in transwell migration and other signaling assays *in vitro* (5, 9) (also see Fig. 10*A*) but as described above, it does not promote cell migration *in vivo* in an intraperitoneal recruitment assay. Moreover, it blocks the ability of WT CCL2 in several models of inflammation including ovalbumin-induced lung inflammation (52), experimental autoimmune encephalomyelitis (a murine model of multiple sclerosis) (52), and rheumatoid arthritis (53). However, the mechanism has never been entirely clear (52). Because CCL2(P8A) binds less tightly to GAGs than WT CCL2, but maintains full capacity to activate receptor (9), its anti-inflammatory activity may be mechanistically similar to the 40s loop CCL7 GAG mutant in systemically desensitizing receptor, in this case CCR2, on migrating cells. By contrast, when injected *in vivo* for visualization by intravital microscopy, CCL2(P8A) was able to promote adhesion and transmigration as efficiently as the WT protein, presumably due to local administration of a low dose of chemokine, which would be less likely to promote systemic desensitization (54).

Another unexpected observation from these studies was that the GAG-bound oligomeric state of CCL2 was dependent on the type of GAG (heparin *versus* HS). Previously, we showed that heparin shifts the equilibrium of CCL2 from a dimer in solution to a tetramer in the presence of the GAG because in the context of a tetramer, the GAG-binding epitope of the monomer coalesces into a large linear basic patch (Fig. 2*C*), which is complementary to the high sulfation density of heparin (11). By contrast, in the context of dimeric CCL2, two identical symmetry-related GAG-binding epitopes occupy opposite ends of the dimer structure (Fig. 2*D*), and may provide a more complementary binding surface for HS because of the domain structure of HS, which consists of sulfated domains separated by unsulfated *N*-acetylated domains, or possibly bridge two adjacent HS chains as depicted in Fig. 11 (*left*). Indeed, cross-linking studies support the notion that HS favors dimers, whereas tetramers and higher order oligomer species are formed in the presence of heparin (Fig. 2). A dimer model has also previously been suggested for MIP-1α/CCL3 binding to HS, which is consistent with the overall similar dimeric architecture of these two CC chemokines (55). Again, by contrast, CCL7 seems to bind GAGs as a monomer, independent of the type of the GAG.

CONCLUSION

Taken together, the present data indicate that CCL2 and CCL7 utilize different mechanisms for GAG binding. Despite some common GAG-binding epitopes, CCL2 requires oligomerization but CCL7 does not because it has a higher density of GAG-binding epitopes within the monomeric subunit, which also may make CCL7 a more promiscuous GAG binder than CCL2. Although there is little literature to support this idea, it is conceivable that these differences in GAG binding and oligomerization propensities could contribute to either different biological/non-redundant functions, or that the regulation of these chemokines through their respective GAG binding and oligomerization properties provide some biological advantage in certain inflammatory settings. For example, CCL2 oligomerizes but only the monomeric form binds and activates CCR2 (9, 56); thus concentrations of CCL2 that promote homo-oligomerization or hetero-oligomerization with other chemokines (35) could inhibit CCR2 activation. By contrast, CCL7 would not be subject to negative regulation by oligomerization. We also demonstrate the utility of hydroxyl radical footprinting for identifying GAG-binding epitopes on proteins. CCL7 is a small protein and this strategy would clearly be even more beneficial for mapping GAG-binding epitopes of large proteins to reduce the number of mutants needed for validation.

Acknowledgments—We gratefully acknowledge Dr. Parminder Kaur for assistance with ProtMapMS data analysis. The National Synchrotron Light Source at Brookhaven National Laboratory is supported by the Department of Energy Contract DE-AC02-98CH10886.

REFERENCES

1. Soria, G., Lebel-Haziv, Y., Ehrlich, M., Meshel, T., Suez, A., Avezov, E., Rozenberg, P., and Ben-Baruch, A. (2012) Mechanisms regulating the secretion of the promalignancy chemokine CCL5 by breast tumor cells: CCL5's 40s loop and intracellular glycosaminoglycans. *Neoplasia* **14,** 1–19
2. Bishop, J. R., Schuksz, M., and Esko, J. D. (2007) Heparan sulphate proteoglycans fine-tune mammalian physiology. *Nature* **446,** 1030–1037
3. Wang, L., Fuster, M., Sriramarao, P., and Esko, J. D. (2005) Endothelial heparan sulfate deficiency impairs L-selectin- and chemokine-mediated neutrophil trafficking during inflammatory responses. *Nat. Immunol.* **6,** 902–910
4. Roscic-Mrkic, B., Fischer, M., Leemann, C., Manrique, A., Gordon, C. J., Moore, J. P., Proudfoot, A. E., and Trkola, A. (2003) RANTES (CCL5) uses the proteoglycan CD44 as an auxiliary receptor to mediate cellular activation signals and HIV-1 enhancement. *Blood* **102,** 1169–1177
5. Proudfoot, A. E., Handel, T. M., Johnson, Z., Lau, E. K., LiWang, P., Clark-Lewis, I., Borlat, F., Wells, T. N., and Kosco-Vilbois, M. H. (2003) Glycosaminoglycan binding and oligomerization are essential for the *in vivo* activity of certain chemokines. *Proc. Natl. Acad. Sci. U.S.A.* **100,** 1885–1890
6. Peterson, F. C., Elgin, E. S., Nelson, T. J., Zhang, F., Hoeger, T. J., Linhardt, R. J., and Volkman, B. F. (2004) Identification and characterization of a glycosaminoglycan recognition element of the C chemokine lymphotactin. *J. Biol. Chem.* **279,** 12598–12604
7. Ali, S., Robertson, H., Wain, J. H., Isaacs, J. D., Malik, G., and Kirby, J. A. (2005) A non-glycosaminoglycan-binding variant of CC chemokine ligand 7 (monocyte chemoattractant protein-3) antagonizes chemokine-mediated inflammation. *J. Immunol.* **175,** 1257–1266
8. O'Boyle, G., Mellor, P., Kirby, J. A., and Ali, S. (2009) Anti-inflammatory therapy by intravenous delivery of non-heparan sulfate-binding CXCL12. *FASEB J.* **23,** 3906–3916
9. Paavola, C. D., Hemmerich, S., Grunberger, D., Polsky, I., Bloom, A., Freedman, R., Mulkins, M., Bhakta, S., McCarley, D., Wiesent, L., Wong, B., Jarnagin, K., and Handel, T. M. (1998) Monomeric monocyte chemoattractant protein-1 (MCP-1) binds and activates the MCP-1 receptor CCR2B. *J. Biol. Chem.* **273,** 33157–33165
10. Rajarathnam, K., Sykes, B. D., Kay, C. M., Dewald, B., Geiser, T., Baggiolini, M., and Clark-Lewis, I. (1994) Neutrophil activation by monomeric interleukin-8. *Science* **264,** 90–92
11. Lau, E. K., Paavola, C. D., Johnson, Z., Gaudry, J.-P., Geretti, E., Borlat, F.,

Kungl, A. J., Proudfoot, A. E., and Handel, T. M. (2004) Identification of the glycosaminoglycan binding site of the CC chemokine, MCP-1: implications for structure and function *in vivo*. *J. Biol. Chem.* **279,** 22294–22305
12. Poluri, K. M., Joseph, P. R., Sawant, K. V., and Rajarathnam, K. (2013) Molecular basis of glycosaminoglycan heparin binding to the chemokine CXCL1 dimer. *J. Biol. Chem.* **288,** 25143–25153
13. Ziarek, J. J., Veldkamp, C. T., Zhang, F., Murray, N. J., Kartz, G. A., Liang, X., Su, J., Baker, J. E., Linhardt, R. J., and Volkman, B. F. (2013) Heparin oligosaccharides inhibit chemokine (CXC motif) ligand 12 (CXCL12) cardioprotection by binding orthogonal to the dimerization interface, promoting oligomerization, and competing with the chemokine (CXC motif) receptor 4 (CXCR4) N terminus. *J. Biol. Chem.* **288,** 737–746
14. Koopmann, W., Ediriwickrema, C., and Krangel, M. S. (1999) Structure and function of the glycosaminoglycan binding site of chemokine macrophage-inflammatory protein-1β. *J. Immunol.* **163,** 2120–2127
15. Koopmann, W., and Krangel, M. S. (1997) Identification of a glycosaminoglycan-binding site in chemokine macrophage inflammatory protein-1α. *J. Biol. Chem.* **272,** 10103–10109
16. Proudfoot, A. E., Fritchley, S., Borlat, F., Shaw, J. P., Vilbois, F., Zwahlen, C., Trkola, A., Marchant, D., Clapham, P. R., and Wells, T. N. (2001) The BB*X*B motif of RANTES is the principal site for heparin binding and controls receptor selectivity. *J. Biol. Chem.* **276,** 10620–10626
17. Kuschert, G. S., Hoogewerf, A. J., Proudfoot, A. E., Chung, C. W., Cooke, R. M., Hubbard, R. E., Wells, T. N., and Sanderson, P. N. (1998) Identification of a glycosaminoglycan binding surface on human interleukin-8. *Biochemistry* **37,** 11193–11201
18. Severin, I. C., Gaudry, J.-P., Johnson, Z., Kungl, A., Jansma, A., Gesslbauer, B., Mulloy, B., Power, C., Proudfoot, A. E., and Handel, T. (2010) Characterization of the chemokine CXCL11-heparin interaction suggests two different affinities for glycosaminoglycans. *J. Biol. Chem.* **285,** 17713–17724
19. Salanga, C. L., and Handel, T. M. (2011) Chemokine oligomerization and interactions with receptors and glycosaminoglycans: the role of structural dynamics in function. *Exp. Cell Res.* **317,** 590–601
20. Ren, M., Guo, Q., Guo, L., Lenz, M., Qian, F., Koenen, R. R., Xu, H., Schilling, A. B., Weber, C., Ye, R. D., Dinner, A. R., and Tang, W.-J. (2010) Polymerization of MIP-1 chemokine (CCL3 and CCL4) and clearance of MIP-1 by insulin-degrading enzyme. *EMBO J.* **29,** 3952–3966
21. Wang, X., Watson, C., Sharp, J. S., Handel, T. M., and Prestegard, J. H. (2011) Oligomeric structure of the chemokine CCL5/RANTES from NMR, MS, and SAXS data. *Structure* **19,** 1138–1148
22. Allen, S. J., Crown, S. E., and Handel, T. M. (2007) Chemokine: receptor structure, interactions, and antagonism. *Annu. Rev. Immunol.* **25,** 787–820
23. Richardson, R. M., Pridgen, B. C., Haribabu, B., and Snyderman, R. (2000) Regulation of the human chemokine receptor CCR1. Cross-regulation by CXCR1 and CXCR2. *J. Biol. Chem.* **275,** 9201–9208
24. Blanpain, C., Migeotte, I., Lee, B., Vakili, J., Doranz, B. J., Govaerts, C., Vassart, G., Doms, R. W., and Parmentier, M. (1999) CCR5 binds multiple CC-chemokines: MCP-3 acts as a natural antagonist. *Blood* **94,** 1899–1905
25. Menten, P., Wuyts, A., and Van Damme, J. (2001) Monocyte chemotactic protein-3. *Eur. Cytokine Netw.* **12,** 554–560
26. Yu, Y., Sweeney, M. D., Saad, O. M., Crown, S. E., Hsu, A. R., Handel, T. M., and Leary, J. A. (2005) Chemokine-glycosaminoglycan binding: specificity for CCR2 ligand binding to highly sulfated oligosaccharides using FTICR mass spectrometry. *J. Biol. Chem.* **280,** 32200–32208
27. Kim, K. S., Rajarathnam, K., Clark-Lewis, I., and Sykes, B. D. (1996) Structural characterization of a monomeric chemokine: monocyte chemoattractant protein-3. *FEBS Lett.* **395,** 277–282
28. Catanzariti, A.-M., Soboleva, T. A., Jans, D. A., Board, P. G., and Baker, R. T. (2004) An efficient system for high-level expression and easy purification of authentic recombinant proteins. *Protein Sci.* **13,** 1331–1339
29. Kiselar, J. G., Janmey, P. A., Almo, S. C., and Chance, M. R. (2003) Structural analysis of gelsolin using synchrotron protein footprinting. *Mol. Cell. Proteomics* **2,** 1120–1132
30. Kaur, P., Kiselar, J. G., and Chance, M. R. (2009) Integrated algorithms for high-throughput examination of covalently labeled biomolecules by structural mass spectrometry. *Anal. Chem.* **81,** 8141–8149
31. Takamoto, K., and Chance, M. R. (2006) Radiolytic protein footprinting with mass spectrometry to probe the structure of macromolecular complexes. *Annu. Rev. Biophys. Biomol. Struct.* **35,** 251–276
32. Tanino, Y., Coombe, D. R., Gill, S. E., Kett, W. C., Kajikawa, O., Proudfoot, A. E., Wells, T. N., Parks, W. C., Wight, T. N., Martin, T. R., and Frevert, C. W. (2010) Kinetics of chemokine-glycosaminoglycan interactions control neutrophil migration into the airspaces of the lungs. *J. Immunol.* **184,** 2677–2685
33. Schenauer, M. R., Yu, Y., Sweeney, M. D., and Leary, J. A. (2007) CCR2 chemokines bind selectively to acetylated heparan sulfate octasaccharides. *J. Biol. Chem.* **282,** 25182–25188
34. Lubkowski, J., Bujacz, G., Boqué, L., Domaille, P. J., Handel, T. M., and Wlodawer, A. (1997) The structure of MCP-1 in two crystal forms provides a rare example of variable quaternary interactions. *Nat. Struct. Biol.* **4,** 64–69
35. Crown, S. E., Yu, Y., Sweeney, M. D., Leary, J. A., and Handel, T. M. (2006) Heterodimerization of CCR2 chemokines and regulation by glycosaminoglycan binding. *J. Biol. Chem.* **281,** 25438–25446
36. Guan, J.-Q., Takamoto, K., Almo, S. C., Reisler, E., and Chance, M. R. (2005) Structure and dynamics of the actin filament. *Biochemistry* **44,** 3166–3175
37. Hileman, R. E., Fromm, J. R., Weiler, J. M., and Linhardt, R. J. (1998) Glycosaminoglycan-protein interactions: definition of consensus sites in glycosaminoglycan binding proteins. *Bioessays* **20,** 156–167
38. Krohn, S. C., Bonvin, P., and Proudfoot, A. E. (2013) CCL18 exhibits a regulatory role through inhibition of receptor and glycosaminoglycan binding. *PLoS ONE* **8,** e72321
39. Veldkamp, C. T., Peterson, F. C., Pelzek, A. J., and Volkman, B. F. (2005) The monomer-dimer equilibrium of stromal cell-derived factor-1 (CXCL 12) is altered by pH, phosphate, sulfate, and heparin. *Protein Sci.* **14,** 1071–1081
40. Jansma, A. L., Kirkpatrick, J. P., Hsu, A. R., Handel, T. M., and Nietlispach, D. (2010) NMR analysis of the structure, dynamics, and unique oligomerization properties of the chemokine CCL27. *J. Biol. Chem.* **285,** 14424–14437
41. Kawamura, T., Stephens, B., Qin, L., Yin, X., Dores, M. R., Smith, T. H., Grimsey, N., Abagyan, R., Trejo, J., Kufareva, I., Fuster, M. M., Salanga, C. L., and Handel, T. M. (2014) A general method for site-specific fluorescent labeling of recombinant chemokines. *PLoS ONE* **9,** e81454
42. Goger, B., Halden, Y., Rek, A., Mösl, R., Pye, D., Gallagher, J., and Kungl, A. J. (2002) Different affinities of glycosaminoglycan oligosaccharides for monomeric and dimeric interleukin-8: a model for chemokine regulation at inflammatory sites. *Biochemistry* **41,** 1640–1646
43. Kuschert, G. S., Coulin, F., Power, C. A., Proudfoot, A. E., Hubbard, R. E., Hoogewerf, A. J., and Wells, T. N. (1999) Glycosaminoglycans interact selectively with chemokines and modulate receptor binding and cellular responses. *Biochemistry* **38,** 12959–12968
44. Kuschert, G. S., Hubbard, R. E., Power, C. A., Wells, T. N., and Hoogewerf, A. J. (1997) Solid-phase binding assay to study interaction of chemokines with glycosaminoglycans. *Methods Enzymol.* **287,** 369–378
45. Sadir, R., Baleux, F., Grosdidier, A., Imberty, A., and Lortat-Jacob, H. (2001) Characterization of the stromal cell-derived factor-1α-heparin complex. *J. Biol. Chem.* **276,** 8288–8296
46. Hamel, D. J., Sielaff, I., Proudfoot, A. E. I., and Handel, T. M. (2009) *Interactions of Chemokines with Glycosaminoglycans*, 1st Ed., c2009, pp. 71–102, Elsevier Inc., New York
47. Charvátová, O., Foley, B. L., Bern, M. W., Sharp, J. S., Orlando, R., and Woods, R. J. (2008) Quantifying protein interface footprinting by hydroxyl radical oxidation and molecular dynamics simulation: application to galectin-1. *J. Am. Soc. Mass Spectrom.* **19,** 1692–1705
48. Kiselar, J. G., Mahaffy, R., Pollard, T. D., Almo, S. C., and Chance, M. R. (2007) Visualizing Arp2/3 complex activation mediated by binding of ATP and WASp using structural mass spectrometry. *Proc. Natl. Acad. Sci. U.S.A.* **104,** 1552–1557
49. Laguri, C., Sadir, R., Rueda, P., Baleux, F., Gans, P., Arenzana-Seisdedos, F., and Lortat-Jacob, H. (2007) The novel CXCL12γ isoform encodes an unstructured cationic domain which regulates bioactivity and interaction

with both glycosaminoglycans and CXCR4. *PLoS ONE* **2,** e1110
50. Saesen, E., Sarrazin, S., Laguri, C., Sadir, R., Maurin, D., Thomas, A., Imberty, A., and Lortat-Jacob, H. (2013) Insights into the mechanism by which interferon-γ basic amino acid clusters mediate protein binding to heparan sulfate. *J. Am. Chem. Soc.* **135,** 9384–9390
51. Gangavarapu, P., Rajagopalan, L., Kolli, D., Guerrero-Plata, A., Garofalo, R. P., and Rajarathnam, K. (2012) The monomer-dimer equilibrium and glycosaminoglycan interactions of chemokine CXCL8 regulate tissue-specific neutrophil recruitment. *J. Leukocyte Biol.* **91,** 259–265
52. Handel, T. M., Johnson, Z., Rodrigues, D. H., Dos Santos, Dos, A. C., Cirillo, R., Muzio, V., Riva, S., Mack, M., Déruaz, M., Borlat, F., Vitte, P.-A., Wells, T. N., Teixeira, M. M., and Proudfoot, A. E. (2008) An engineered monomer of CCL2 has anti-inflammatory properties emphasizing the importance of oligomerization for chemokine activity *in vivo*. *J. Leukocyte Biol.* **84,** 1101–1108
53. Shahrara, S., Proudfoot, A. E., Park, C. C., Volin, M. V., Haines, G. K., Woods, J. M., Aikens, C. H., Handel, T. M., and Pope, R. M. (2008) Inhibition of monocyte chemoattractant protein-1 ameliorates rat adjuvant-induced arthritis. *J. Immunol.* **180,** 3447–3456
54. Tan, J. H., Ludeman, J. P., Wedderburn, J., Canals, M., Hall, P., Butler, S. J., Taleski, D., Christopoulos, A., Hickey, M. J., Payne, R. J., and Stone, M. J. (2013) Tyrosine sulfation of chemokine receptor CCR2 enhances interactions with both monomeric and dimeric forms of the chemokine monocyte chemoattractant protein-1 (MCP-1). *J. Biol. Chem.* **288,** 10024–10034
55. Stringer, S. E., Forster, M. J., Mulloy, B., Bishop, C. R., Graham, G. J., and Gallagher, J. T. (2002) Characterization of the binding site on heparan sulfate for macrophage inflammatory protein 1α. *Blood* **100,** 1543–1550
56. Tan, J. H., Canals, M., Ludeman, J. P., Wedderburn, J., Boston, C., Butler, S. J., Carrick, A. M., Parody, T. R., Taleski, D., Christopoulos, A., Payne, R. J., and Stone, M. J. (2012) Design and receptor interactions of obligate dimeric mutant of chemokine monocyte chemoattractant protein-1 (MCP-1). *J. Biol. Chem.* **287,** 14692–14702
57. Sarrazin, S., Lamanna, W. C., and Esko, J. D. (2011) Heparan sulfate proteoglycans. *Cold Spring Harbor Perspectives Biol.* **3,** a004952-a004952